No. 4/2014

HIDRAULICA

HYDRAULICS-PNEUMATICS-TRIBOLOGY-ECOLOGY-SENSORICS-MECHATRONICS

ISSN 1453 - 7303
ISSN-L 1453 - 7303

CONTENTS

- **EDITORIAL: JUMATATEA PLINA / HALF FULL** 5 - 6
Petrin DRUMEA

- **DEVELOPMENT OF A TEST BENCH FOR ANALYSIS OF THE SUPPLY PRESSURE VARIATION IN HYDRAULIC SYSTEMS** 7 - 17
Prof. MSc. R.M. Castro, Prof. MSc. J.M. Neto, Y.M. Morona, K. Machado, Prof. Dr. A. S. Rocha

- **EXPERIMENTAL RESEARCH ON VISCOUS FLUID FLOW THROUGH SEALING LABYRINTHS** 18 - 21
Lecturer PhD. Eng. Sanda BUDEA, PhD.St. Eng. Stefan SIMIONESCU

- **MECHATRONIC DRIVE SYSTEM FOR CLEANING MACHINE OF PHOTOVOLTAIC PANELS** 22 - 26
PhD. eng. Radu RADOI, PhD. eng. Marian BLEJAN, PhD. St. eng. Ioana ILIE

- **INFLUENCE OF NITRIDING THERMOCHEMICAL TREATMENTS UPON CAVITATION EROSION RESISTANCE OF DUPLEX X2CrNiMoN22-5-3 STAINLESS STEELS** 27 - 33
Assist. PhD.eng. Lavinia Madalina MICU, Student Dorin BORDEASU,
Prof. PhD.eng. Ilare BORDEASU, Assoc. Prof. PhD.eng. Mihaela POPESCU,
PhD.eng. Octavian Victor OANCA, Lecturer PhD.eng. Sebastian Titus DUMA

- **TRIBOLOGY PERSPECTIVE ON SEATBELT PRETENSIONING SYSTEM Tribology perspective on seatbelt pretensioning mechanism** 34 - 41
Dipl.eng. Paul IMRE

- **OPTIMIZING THE ENERGY CONSUMPTION OF AN INDUSTRIAL WATER-SUPPLY PUMP SYSTEM BY ENSURING AN OPTIMAL FLOW RATE** 42 - 50
Prof. PhD Gencho POPOV, PhD Boris KOSTOV, PhD Miglena HRISTOVA,
Asc. Prof. Donka IVANOVA, Asc. Prof. Anka KRUSTEVA

- **TWO OPERATING MODES ELECTRO-HYDRAULIC SERVO VALVE** 51 - 55
PhD. eng. Teodor Costinel POPESCU, Dipl.eng. Alina Iolanda POPESCU

- **EXPERIMENTAL RESEARCH ON HIGH EFFICIENCY SOLAR AIR HEATING COLLECTORS** 56 - 60
Prof. Ph.D. Adrian CIOCANEA, Lect. Ph.D. Dorin Laurenţiu BUREŢEA

Published by:
Hydraulics & Pneumatics Research Institute, Bucharest-Romania
Address: 14 Cuţitul de Argint, district 4, Bucharest, cod 040557, ROMANIA
Phone: +40 21 336 39 90; +40 21 336 39 91 ; Fax:+40 21 337 30 40 ;
E-mail: ihp@fluidas.ro
Web: www.ihp.ro

with support of:
National Professional Association of Hydraulics and Pneumatics in Romania - FLUIDAS
E-mail: fluidas@fluidas.ro
Web: www.fluidas.ro

HIDRAULICA Magazine is indexed in the international databases:

HIDRAULICA Magazine is indexed in the Romanian Editorial Platform:

ISSN 1453 – 7303; ISSN – L 1453 – 7303

EDITORIAL

JUMATATEA PLINA

Dr.ing. Petrin DRUMEA
DIRECTOR DE PUBLICATIE

Despre hidraulica din tara noastra am vorbit adesea, ne-am dat cu parerea de multe ori, am tot scos in evidenta problemele domeniului si foarte rar si destul de putin am subliniat si partile bune. In acest editorial voi incerca sa scot in evidenta partea plina a paharului, evitand sa critic multele lucruri care ma deranjeaza.

Primul subdomeniu este cel al cercetarii si proiectarii echipamentelor si sistemelor hidraulice si pneumatice, care a supravietuit ultimilor ani. Exista in tara cateva centre care au obtinut si obtin rezultate interesante mai ales in zona sistemelor.
In acest sens sunt de remarcat eforturile Institutului de Hidraulica si Pneumatica din Bucuresti, Centrelor de cercetare din Universitatile Tehnice din Cluj-Napoca, din Timisoara, din Iasi, din Constanta si din Bucuresti (Politehnica si Universitatea Tehnica de Constructii), unde activeaza specialisti de inalta calificare. Tot in aceste centre s-au creat laboratoare moderne de cercetare si de testare care pot asigura o activitate de inalt nivel. Tot aici trebuie remarcata si sustinerea forurilor statale care in aceste perioade grele au asigurat un minim de fonduri cu care s-a reusit mentinerea unor mici entitati de cercetare, dezvoltare, inovare. Sigur ca sunt multe de spus despre repartizarea acestor fonduri, dar in acest editorial discutam numai partea buna a lucrurilor.

Al doilea subdomeniu este cel al productiei, care in ultima perioada a intrat si in vizorul marilor producatori internationali, ceea ce va conduce in final la refacerea unei productii de calitate si intr-o cantitate care sa conteze atat pe plan national cat si pe plan international. Este de asemenea de remarcat cresterea numarului si nivelului tehnic al instalatiilor care echipeaza utilaje complexe din toate domeniile economiei. Este interesant de stiut ca desi exista imaginea unui dezastru in productie, exista inca export de hidraulica, chiar si la nivelul echipamentelor, mai ales in zona cilindrilor si pompelor cu roti dintate. Este de subliniat faptul ca inca exista in tara un numar suficient de mare de specialisti in probleme de productie si foarte important ca sunt un numar apreciabil de tineri in randul acestora, ceea ce ne face sa apreciem ca Universitatile sunt destul de active si mai ales orientate din ce in ce mai mult pe cerintele pietei.

Al treilea subdomeniu si ultimul analizat in acest editorial il reprezinta grupul mare de reprezentante ale marilor firme de hidraulica si pneumatica din intreaga lume. Faptul ca aceste firme au angajat pe langa tineri si specialisti cu vechi state de serviciu in domeniu a facut ca pe langa activitatea de vanzare si consultanta sa isi dezvolte si o serioasa munca de conceptie si productie. Cursurile de perfectionare ale acestor firme, adaugate cursurilor organizate de Institutul de Hidraulica si Pneumatica, au condus la cresterea numarului de specialist tineri in domeniu si la cunoasterea noutatilor domeniului de catre specialistii mai in varsta.

Trebuie remarcat ca in ultima perioada a crescut numarul de teme de nivel inalt cu care economia nationala se adreseaza specialistilor romani si mai ales faptul ca realizarile acestora sunt in conformitate cu cerintele utilajelor moderne.

In final va doresc multa sanatate si sa retineti ca hidraulica de la noi inca traieste.

EDITORIAL

HALF FULL

Ph.D.Eng. Petrin DRUMEA
MANAGER OF PUBLICATION

About hydraulics in our country we have spoken often, often stated our opinion, and pointed out the problems of this activity field, but very rarely and quite a bit have emphasized also the good stuff. In this editorial I will try to highlight the half full glass, avoiding to criticize many things that bother me.

The first subfield is that of research and design of hydraulic and pneumatic equipment and systems, which survived recent years. There are few centers in the country that have achieved and still achieve interesting results especially in the area of systems.
In this respect it is worth mentioning the efforts of Hydraulics and Pneumatics Research Institute in Bucharest, of Research Centers in Technical Universities of Cluj-Napoca, Timisoara, Iasi, Constanta and Bucharest ("Politehnica" and the University of Civil Engineering), wherein highly qualified specialists conduct their work. Also in these centers there have been established modern research and test laboratories, which can ensure a high-level activity. Here it should be also noted the support of the state forums that in these hard times have provided a minimum of funds thanks to which it was possible to maintain alive small research, development and innovation entities. Of course there is much to say about the distribution of these funds, but this editorial discusses only the bright side.

The second subfield is that of manufacturing, which lately came in sight of large international manufacturers, which will eventually lead to the restoration of quality production and in a quantity that matters aboth nationally and internationally. It is also noteworthy the increasing in number and improvement of technical level of installations equipping complex machines from all areas of the economy. It is interesting to note that although there is the image of a disaster in production, there are still exports of hydraulic parts, even at the level of equipment, especially in cylinders and gear pumps. It should be pointed out that in Romania there are still a sufficient number of experts in the production problems, and is very important that there are a considerable number of young people among them, which leads us to consider that universities are quite active and especially they are increasingly targeting more the market demands.

The third subfield and last reviewed in this editorial is the large group of representatives of major companies active in hydraulics and pneumatics from around the world. The fact that these companies have employed besides young people also older specialists in the field has made them that in addition to sales and consulting activities to develop also a solid design and manufacturing activity. Training courses of those companies, complementary to courses organized by Hydraulics and Pneumatics Research Institute, led to an increasing number of young professionals in the field and also to knowledge updates for the older experts.

It should be noted that lately there has increased the number of high-level topics with which the national economy addresses Romanian specialists, and especially the fact that their achievements are complying with the requirements of modern equipment.

Finally, I wish you good health and keep in mind that Hydraulics in our country is still alive.

DEVELOPMENT OF A TEST BENCH FOR ANALYSIS OF THE SUPPLY PRESSURE VARIATION IN HYDRAULIC SYSTEMS

Prof. MSc. R.M. Castro[1], Prof. MSc. J.M. Neto[2], Y.M. Morona[3], K. Machado[4], Prof. Dr. A. S. Rocha[5]

[1,2,3,4] School of Engineering, Department of Mechanical Engineering and Automation, Faculty SATC, Criciúma, SC (Brazil), Laboratory Automation and Simulation of Hydraulic and Pneumatic Systems – LASPHI
[5] Federal University of Rio Grande do Sul - UFRGS, LdTM, Porto Alegre, RS - Brazil

Abstract: *Hydraulic systems have gained widespread use and applicability to the industrial manufacturing process. Although the hydraulic technology is old, there are many modern applications such as presses, mechanical excavators, backhoes, loaders, forklifts and cranes. However, studies show that the stability of the supply pressure is a determinant for gain efficient of any hydraulic equipment. This study aimed to analyze the characteristics of the variation in supply pressure in a hydraulic system under different conditions of operation, through a test bench. Were first showed constructive and operating characteristics of the major components analyzed, these being the proportional directional valve, pressure relief valve direct operated (relief valve) and the accumulator. Subsequently, addressed the relationship between the operation of the relief valve and the behavior of the supply pressure. In the experiments, the proportional directional valve is subjected to different conditions of pressure difference and aperture alternating also, the use of an accumulator in the circuit. The results show the relation between the operating conditions of the hydraulic circuit and the change in supply pressure.*

Keywords: *Hydraulic System, Pressure Supply, Relief Valve, Tests Bench.*

1. Introduction

Hydraulic systems can be defined as the combination of physical elements conveniently mounted using the fluid as energy transfer and control of forces and movements. Currently great efforts have been made to the development of this technology, due to huge application in all fields of activities, from mining to industrial space. Because of this, highlights that the recent growing interest and need for more industry adequate to meet the market demanding hydraulic systems. These are factors that favor the funding of academic research dedicated to increasing of hydraulics systems knowledge [1], [8].

Most hydraulic systems are equipped with a pressure relief valve (relief valve) that keeps the working pressure of the system (supply pressure) to a predetermined level. This component protects both the hydraulic pump and the electric motor of an excessive increase in system pressure through the partial or total diverting flow provided by the pump [2].

However, due to the static response of the relief valve, supply pressure fluctuations arising from the amendment present the flow passing through it. This change in the working condition of the relief valve is caused, for example, after activate the directional control valve. Depending on the application this behavior should be avoided [3].

In this case, due to the absence of an accumulator, is necessary to work at low speeds so that the variations in flow and therefore the pressure gonna be slower and the pressure control valves are able to maintain the supply pressure constant. The drop in supply pressure directly influences the hydraulic subsystem, hurting following the required hydraulic force, which consequently affects the mechanical subsystem, increasing the trajectory errors of the actuators.

This work will be analyzed the characteristics of fluctuations in supply pressure, checking the relationship between the operating conditions of the hydraulic system, ie opening of the proportional directional valve and loading the cylinder, and the behavior of the relief valve in a hydraulic system, in addition to analyze the influence of the energy accumulator in the behavior of

this phenomenon. In order to get the results, one test bench was developed as will be shown later in the experimental procedure.

2. Literature Review

A hydraulic circuit can be divided into two parts: the circuit of action that encompasses the parts that promote action on the load, and the unit responsible power circuit for supplying hydraulic power for the circuits of activity. The components of a circuit may vary according to the needs of the project in order to adjust them several applications [5].

The valves control and direct the fluid from the pump outlet when returning to the reservoir. The relief valve is almost always the first valve located after the fluid leaves the pump. In a simple circuit probably the second valve used is a directional control valve [6]. The type of pressure control valve is used more relief valve (VA), since that is found on virtually all hydraulic systems. It is a normally closed valve, whose function is to limit the pressure there is a maximum value specified by the partial or total bypass flow from the pump to the reservoir. There are many types of this kind of relief valve, but the concepts discussed in this paper about the VA refer to the pressure relief valve direct operated, Fig.1(a), [7].

The relief valve is basically composed of a shutter which is held in its seat by the effect of the spring force pre-set by a screw. The supply pressure, (P_s) acting on the area of the shutter produces a force (pressing force) that directly opposes the preload force of the compression spring, so that the minimum opening pressure of the valve, (P) is determined the ratio between the strength of pre-compression, (F_m) and (A_p) area subject to the action of supply pressure, (A_p) [1]. The minimum opening pressure (F_m) and strength of pre-spring compression adjustment Fm are given as follows [8], Equation (1) and (2):

$$P_r = \frac{F_m}{A_p} \tag{1}$$

$$F_m = k.x_0 \tag{2}$$

Where:
A_p = Area Shutter subject to the action of pressure P_s
k = Elastic spring constant
x_0 = Course precompression spring

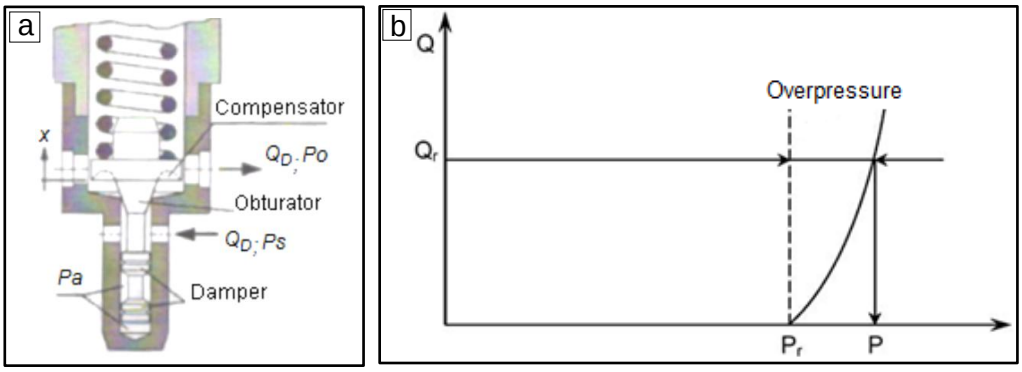

Fig. 1. Principle of operation of the pressure relief valve, direct operated.
(a) the constructive-way [1] and (b) static feature [10]

Any pressure increase above the minimum opening pressure (P_r) causes the shutter to move allowing the adjustment of pressure by diverting flow from the pump to the reservoir. The pressure difference (P_s – P_r) sets the aperture and shutter flow is described following the Bernoulli Equation 3 [9]. The flow through the VA is given by [10]:

$$Q_d = C_d.\omega \frac{A_p}{k}\left(P_s - P_r\right)\sqrt{\frac{2P_s}{\rho}} \tag{3}$$

Where:
Q_d = Flow diverted through the VA
P_s = Supply pressure
P_r = Minimum opening pressure of VA
A_p = Area the shutter subject to supply pressure
k = Spring stiffness
C_d = Discharge coefficient
ω = Proportionality coefficient of orifice area control
ρ = Specific mass of the fluid

According to the behavior described in Figure 1 (b), states that after the opening of the VA, the spring force varies with displacement of the shutter, x. The pressure difference ($P - P_r$) is called pressure, and the greater the displacement of the shutter against the spring (and the greater stiffness of the spring), the larger the effect of the pressure produced by the additional spring force. Thus, it can be stated that the higher the diverted flow overpressure. This shows that the maximum pressure (P), corresponds to the total flow diverted by the VA, (Q_t). When ($P = P_r$), pressure and preload force compression spring are in balance, and with it, the VA remains closed. On business papers the static characteristics of the VA are provided assuming that the flow through this is the independent variable. In Fig.2 where a typical curve of a pressure relief valve provided by manufacturers of this type of valve is shown, it is observed that by modifying the working condition of 1 to 2 due to the change in flow, pressure is affected [10].

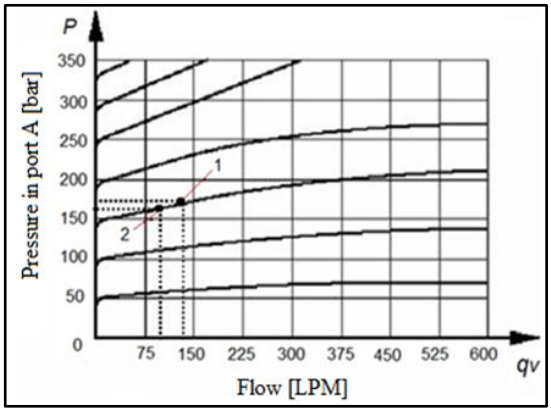

Fig. 2. Typical curve of steady state of a relief valve [4]

3. Experimental Procedure

The hydraulic circuit used in the experiments was assembled in order to simulate the performance of a hydraulic system subjected to an external load. The circuit performance is composed of the following components: Symmetrical through-rod double action, RAGI manufacturer, model RHI01SLBR-TBD200AEXX, the piston diameter of 25 mm, rod diameter 18 mm, 200 mm stroke cylinder; Symmetrical proportional directional valve, direct operated, with pressure balance, without electrical position feedback 4/3, Vickers manufacturer, maximum flow of 1.5 LPM, maximum operating pressure of 120 bar, input signal ± 10 V;

A unit of power used to generate hydropower has the following components: Gear pump with capacity of 3.5 GPM maximum flow rate, operating pressure of 0-60 bar, maximum pressure of 100 bar; Electric motor drive with power of 0.5 HP; Bourdon type pressure gauge to check the

pressure setting; Pressure relief valve direct operated; Energy storage diaphragm, FCH manufacturer, model 108498-01125, gas volume of 0.75 L and a maximum pressure of 210 bar.

3.1 Charging System and Data Acquisition System

For loading of the hydraulic cylinder used a system with steel blocks with a mass of about 20 kg each hydraulic cylinder attached to a cable, moving vertically through a pulley. Through this system the cylinder was fired with three loading conditions, 20, 40 and 60 kg, thus generating three different values of load pressure Pc and knowing that the pressure difference in pressure differential VDP is obtained from the subtraction between the pressure (P_s) supply and pressure load (P_c), modifying the loading caused three conditions of pressure difference pressure differential on the VDP. The pressure in the supply line was measured by a pressure transmitter, GEFRAN manufacturer, model TKN1EB01CMV, measuring range 0-100 bar, and uncertainty ± 0.5 bar, input signal 0-10 V.

The signals measured by the transmitter were sent to a device data acquisition, USB 6008 board. Using LabView (Laboratory Virtual Instrument Engineering Workbench) software, software was developed that allowed the visualization of the signal measured by the pressure transmitter and the generation of graphics necessary to interpret the data acquired by USB 6008 board. The sampling period of the data acquisition system was 1ms.

3.2 Experiments on Bench Study

The experiments performed in the hydraulic circuit based on the displacement of the cylinder by pushing VDP, alternating operating conditions of the circuit performance in each test. For each test run are triggered VDP with different values of control signal (valve opening) and the loading hydraulic cylinder. Values of the step-like command set on the electronic chart to drive the voltage VDP were 4, 6, 8 and 10V (ie, command signals openings or equal to 40, 60, 80, 100%) and loading conditions of the cylinder 20, 40 and 60kg. All tests performed with the conditions described were made with and without the presence of the accumulator in the hydraulic circuit, this control being done through a record of opening and closing of the accumulator system found in the same block safety.

According to Fig. 3, the flow delivered by the pump (Q_b) equals the sum of the flow diverted by the VA (Q_d) and available flow in the hydraulic circuit (Q_c). Therefore, disregarding the compressibility of the fluid, the change in flow (Q_c) controlled by VDP causes the change in flow diverted by the VA.

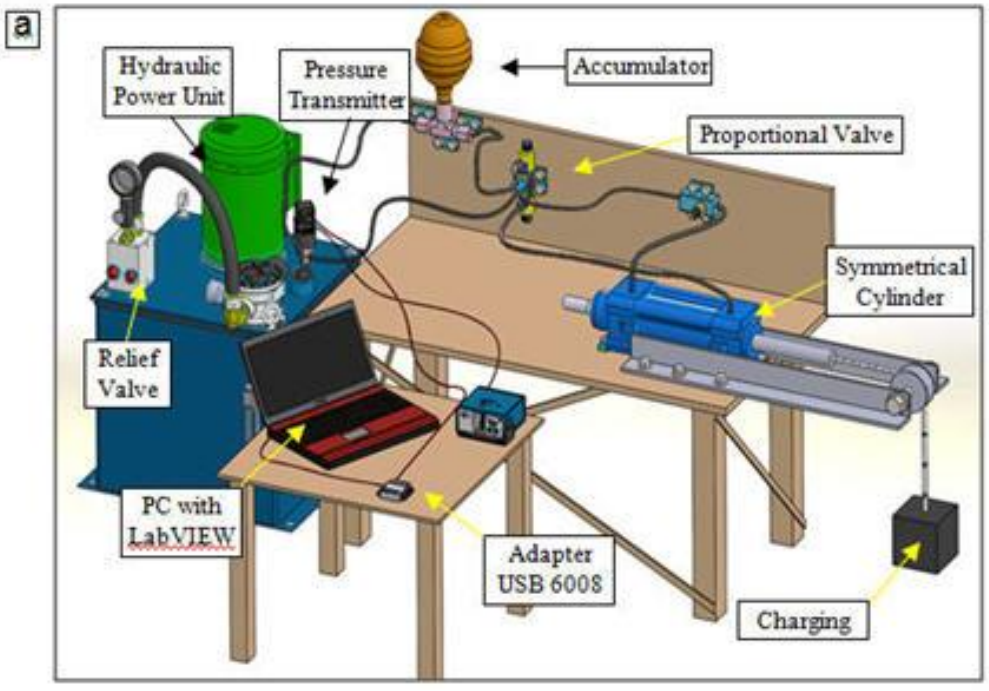

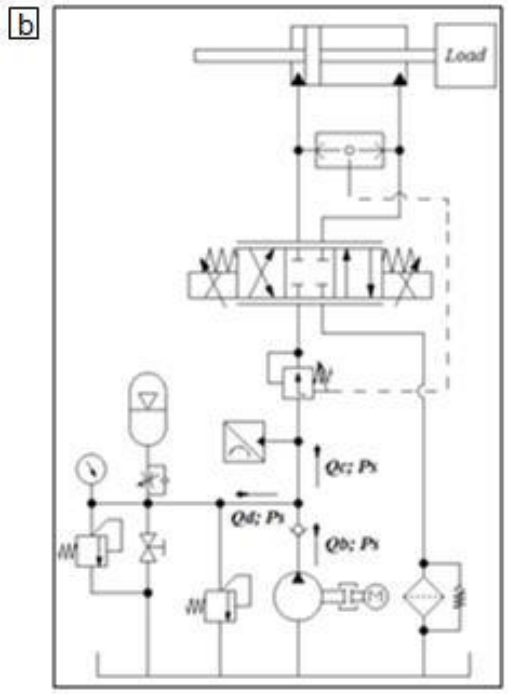

Fig.3 - Bench study: (a) principal components and (b) hydraulic circuit

The minimum opening VDP 40% (command) was determined assuming the internal leakage this happens to be greater for less than this amount opening. The internal leakage in this case could, in the case of this work, compromising the results of the variation of (P_s) because during the performance of a portion of VPD (Q_c) would go directly to the reservoir rather than being diverted by the VA.

The flow rate passing through the VDP used in the experiments has a similar graph to that described in Fig.4 behavior. According to the chart the flow through the VDP is dependent on both the opening signal as the difference in pressure acting on the same, this relation is observed through the characteristic curves for each operating condition. Thus, it was considered that the flow through the VPD was different for each test.

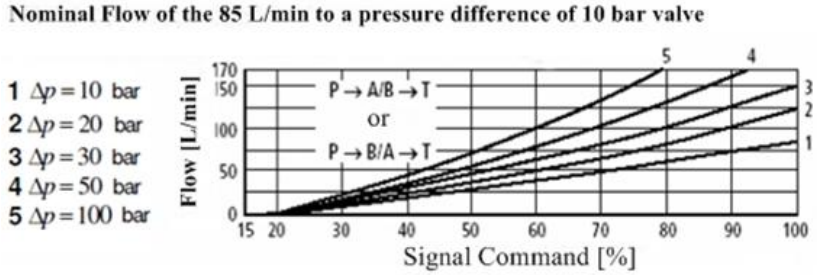

Fig. 4. Graph command signal versus of a flow proportional valve [4].

The supply pressure was initially set at 55 bar ± 1 bar (P_A) because this value is enough to overcome the loading cylinder, where it has been measured by the pressure transmitter for the return of the cylinder, ie in the direction opposite the weight force of the blocks. The cylinder moved in each test approximately 180 mm, avoiding that way, that it reached the end of its stroke and impairs the measurement of supply pressure.

The following are some considerations made regarding the parameters adopted for the experiments: the line pressure of the reservoir was considered zero, pressure loss in piping and circuit components have been disregarded, dynamic Drive VDP was disregarded and force of this friction in the loading system was disregarded.

4. Analysis of Results

According to the relationship between Q_c, Q_b, Q_d (Fig. 3) the opening of the VDP caused the change of flow diverted by the VA, the VA pushing the shutter to move between intermediate positions between its maximum aperture and its closure as the conditions of each test.

The results obtained have demonstrated both the dynamic behavior such as pressure drop P_S based on changes in the working conditions of the control valves used in hydraulic circuit. In the analysis of the results also compared the influence of the action of the accumulator in this phenomenon when this component was used in the circuit.

4.1 Analysis of the Dynamic Behavior of Supply Pressure

For analysis of the dynamic behavior of (P_s) used the results obtained with and without using the accumulator in circuit with a load of 20 kg in the cylinder and openings VDP 40 and 100%. The results were compared in order to be able to examine the relationship between the operation of the circuit components in the behavior of (P_s).

4.1.1 Results without the use of accumulator in the circuit

The Fig. 5 (a) and (b) show the behavior of the roller (P_s) loaded with a mass of 20 kg, and the opening of the VDP 100% and 40%, respectively, without the presence of the accumulator in the circuit.

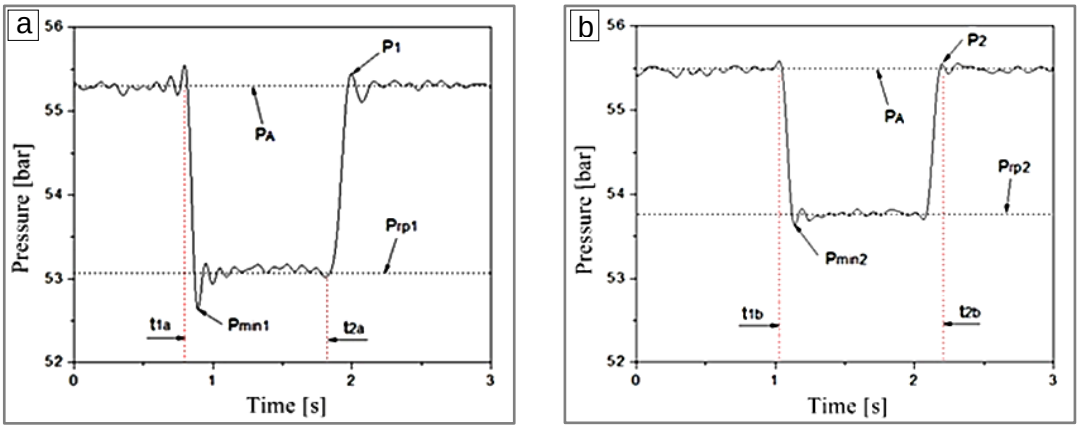

Fig. 5 - Dynamic behavior of supply pressure without the use of the accumulator:
(a) - opening of 100% in the VDP, (b) - opening of 40% in the VDP.

Initially, before the opening of the VDP (P_s) pressure is permanently at the value set at the VA, (P_A), displaying only pulsations arising from the operation of the hydraulic pump. After the activation of the VDP moments (t_{1a}) and (t_{1b}), part of the pump (Q_b) was directed to the circuit by the VDP, the diminishing with this (Q_d) flow diverted by the VA. As noted in both cases, Fig. 5 (a) and (b), after the change in working conditions in the control valves observed pressure drop in supply, where it hovered until it reaches the steady state value and (P_{rp1}) and (P_{rp2}). The oscillation P_S occurred due to the operation of the mechanical device of VA.

The mechanical device that controls the flow through the VA composed of the shutter, the spring and damper tuning, has modeled as a damped spring-mass system behavior [11]. After reduction of the flow VA shutter moves in the direction to decrease the valve opening and due to the delay in the mechanical response of this device, the shutter continued to move causing minimum peaks occur (P_s), and (P_{min1} P_{min2}), Fig.5 (a) and (b), respectively. The effect of damping of this oscillation arises in reaction to movement of the shutter, the restriction to flow through the radial clearance existing between the piston (damper) and the jacket of the damping system [1].

It is observed that in the first case, Fig.5 (a), with the valve fully open (opening = 100%) directed into the flow circuit is greater than in the second case (b) (opening = 40%); causing a further decrease in the flow diverted through the VA. These oscillations in the displacement of the shutter and system pressure, (P_s), result from the disruption of flow and pressure, caused by the sudden increase of pressure in the hydraulic system. Leaving it is concluded that the amplitude of oscillation (P_{min1}, P_s) was higher in the case described in Fig.5 (a) for having generated a disturbance of higher flow in the flow control device VA [1].

The closing moments of the VDP (t_{2a}) and (t_{2b}), caused flow in the circuit passed again being diverted by the VA. Due to the operation of the VA, the rapid increase in flow through this caused the sudden increase in supply pressure, where again it can be seen in both cases the effect of the delay in the response of the device of VA, causing pressure spikes (P_1) and (P_2), as Fig.5 (a) and (b), respectively. After this fact was damped oscillation until the value of the steady pressure initially (P_A) adjusted.

It was noted that in both cases the values (P_1) and (P_2) were very close and relatively low. However, it is known that in cases where the flow and pressure are higher than the values used in the experiments these pressure peaks, as seen in Fig.5 can decrease the pump life.

4.1.2 Results Using the Accumulator in the Circuit

Initially the supply pressure (P_s) is permanently at (P_A) value set in VA, with pulsations again due to the pump. However, as Fig. 6 (a) and 6 (b), the use of the accumulator circuit has caused a change in the dynamic behavior of the supply pressure during the opening of the VDP in relation to the results without the use of the accumulator.

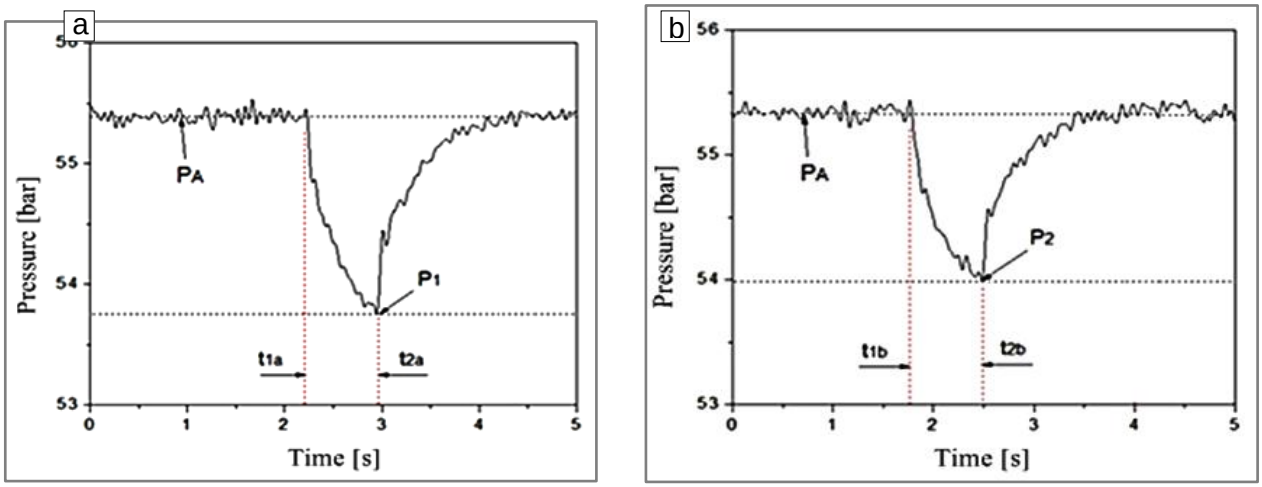

Fig. 6 - Dynamic behavior of supply pressure using the accumulator: (a) - opening of 100% in the VDP, (b) - opening of 40% in the VDP.

In the cases analyzed the supply pressure (P_s) did not show the behavior in steady state during the opening of the VDP may be noted that the fall of (P_s) soon after the opening of the valve occurred gradually until the closing moments of the VDP.

Analyzing the two cases, it was found that after initially opening the VDP in moments t_{1a} and (t_{1b}), part of the flow delivered by the pump (Q_c) was directed to the circuit causing the drop in supply pressure due to operation of VA. From this moment the pressure inside the accumulator became higher than the value of (P_s), allowing the discharge of the pressurized fluid within the accumulator circuit. As part of flow (Q_c) was provided by the accumulator drive, analyzing the (Q_c, Q_b, Q_d) it is concluded that there was less variation in the flow diverted by the VA and, consequently, smaller drops (P_s, P_1 and P_2).

Analyzing the behavior of (P_s), it was noted that his fall was more marked after opening the VDP due to dynamic operation of the accumulator. From the onset of action the accumulator in the circuit, the rate of change of (P_s) decreased characterizing the damping effect generated by the

accumulator. In this way, use of the accumulator prevented sudden drop in (P_s, P_{min1} *and* P_{min2}) oscillations observed in the results was not used in this component, as Fig. 5 (a) and 5 (b).

After the closing of VDP in moments (t_{2a} and t_{2b}), we noticed again the damping effect generated by the accumulator. It was concluded that with the closing of the VDP, part of the pump was absorbed by the battery (energy storage process) rather than being quickly diverted by the VA and thereby avoided the sharp increase in supply pressure. Moreover, it was found that due to the dynamics of operation of the energy accumulation process performed by the accumulator occurred late in restoring the steady state in the set value (P_A). As can be seen, the pulse pump accompanies every curve oscillation (P_A).

4.2 Analysis Fall P_S depending on the operating conditions of the circuit

According to the analysis on the dynamic behavior of (P_s), it was found that the variation of the pressure, ie the pressure drop (P_s) value is related to the decrease in the flow deflected by (Q_d) VA. Decreased flow (Q_d) depends on the increase of the flow (Q_c), resulting from activation of the VDP, so this variation is related to the flow behavior through the VDP. Therefore, the analysis is based on the relationship of the operating conditions of the circuit, the VDP opening and loading of the cylinder, and falling (P_s). Comparing the results, we also analyzed the effect of using the accumulator drop (P_s).

4.2.1 Results P_s drop without using the accumulator circuit

For calculations of the fall of (P_s) each test, we considered the difference between the pressure set on VA (P_A) in continuous and steady state values that occurs during the opening of the VDP, as noted in the analysis of the dynamic behavior (P_s). Each VDP open condition and charging the drum was repeated four times, after this we calculated the average pressure drop between these four values and the standard deviation of these results. The results are shown in Table I.

Tab.I – Results (P_s) drop as a function of the loading cylinder and the control signal VDP without using the accumulator in the circuit

	Loading - 20 kg		**Loading - 40 kg**		**Loading - 60 kg**	
Opening VDP [%]	**Falling P_s [%]**	**Standard Deviation (%)**	**Falling P_s [%]**	**Standard Deviation (%)**	**Falling P_s [%]**	**Standard Deviation (%)**
4	3,34	0,196	3,09	0,102	2,35	0,128
6	3,78	0,147	3,58	0,179	2,74	0,145
8	3,80	0,135	3,61	0,229	2,76	0,121
10	3,83	0,185	3,63	0,204	2,79	0,192

According to Fig.7, the relationship between the increasing opening of the VDP and (P_s) variation for the three load conditions is approximately the same as can be observed in the linear behavior of each condition. This demonstrated that the relationship between the gap and increase the flow through the VDP was approximately the same in all three conditions of the cylinder, as this valve flow behavior observed in Fig.6.

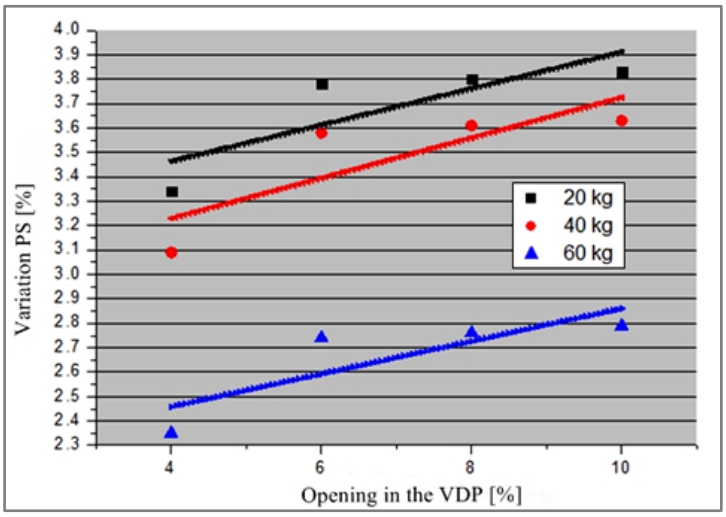

Fig.7 - Variation of (P_s) x aperture VDP (not using the accumulator in the circuit)

Relating to the graph described in Fig.4, the rise of the load pressure decreases the flow through the VDP. The increased load on the cylinder, that is, the load pressure, decreased flow through the VDP generating a smaller change in the flow diverted by VA, and consequently, the less variation in the supply pressure. The decrease in flow by VDP due to increased loading pressure was higher with the loading condition of 60 kg assuming drop (P_s) relatively low compared to other loading conditions.

4.2.2 Analysis of the drop P_s using the battery in the circuit

The variation of (P_s) using the battery in the circuit is calculated based on the values of (P_A) steady state peak and minimum pressure (as Fig. 8). Again, each of the VDP open condition and charging the drum was repeated four times, after that calculated the mean pressure drop from these four values and the standard deviation of these results. The results are shown in Table II.

Tab.II - Results of (P_s) drop as a function of the loading cylinder and the control signal VDP, using the battery in the circuit.

	Loading - 20 kg		Loading - 40 kg		Loading - 60 kg	
Opening VDP [%]	**Falling P_s [%]**	**Standard Deviation (%)**	**Falling P_s [%]**	**Standard Deviation (%)**	**Falling P_s [%]**	**Standard Deviation (%)**
4	2,39	0,187	2,33	0,114	2,09	0,113
6	2,79	0,191	2,74	0,147	2,42	0,156
8	2,81	0,162	2,75	0,149	2,43	0,132
10	2,84	0,148	2,78	0,163	2,51	0,109

As discussed in section 4.1.2, the use of accumulator caused a lower minimum peak pressure in the supply. Figure 8 shows the values were lower drops (P_s) using the battery in the circuit. Comparing the linear behavior with the results without using the battery, it is noticed that in this case the relationship between openness and the fall of the VDP (P_s) was higher.

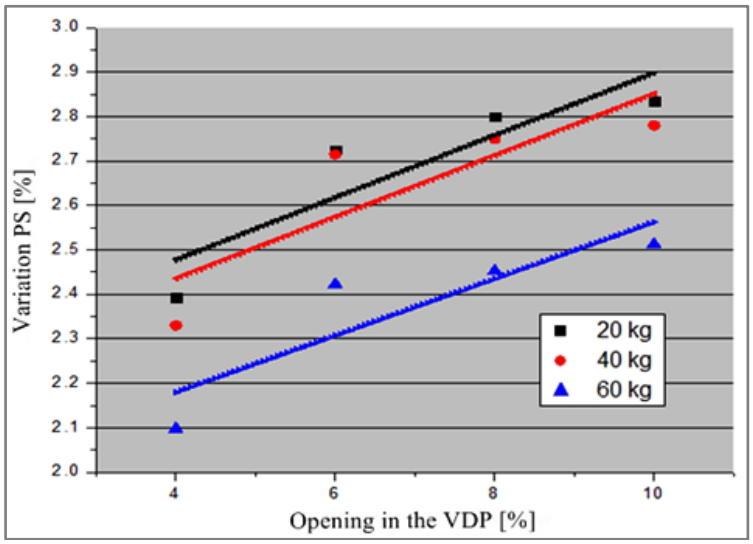

Fig.8 - Variation of (P_S) x opening VDP (using the accumulator in the circuit).

The Fig.9 shows that the reduction in drop (P_S) taken by accumulator was higher in conditions with mass loading of 20 and 40 kg. This fact means that the function of accumulator in the fall of compensation (P_S) was more effective under conditions in which there was greater variation in pressure (P_S), ie, the loadings of 20 and 40 kg in the cylinder, as seen in the results shown in Fig.7.

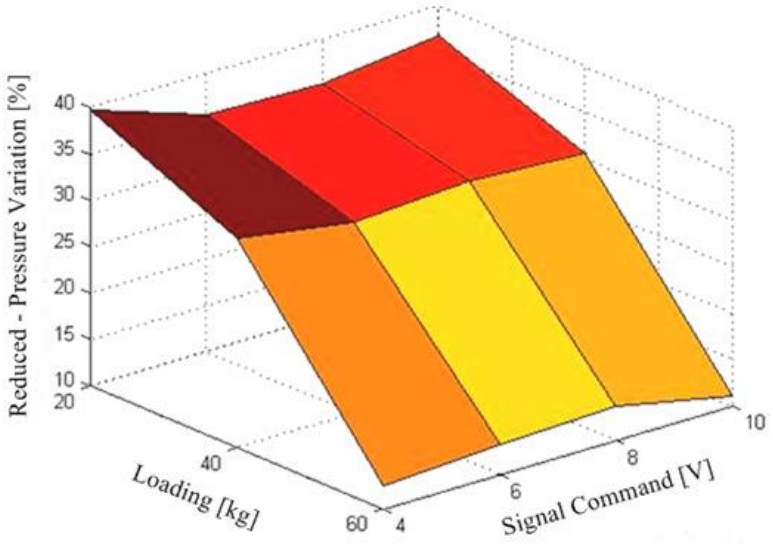

Fig.9 - Reduction of variation ie, the loadings (P_S) from use of the accumulator

5. Final Considerations

With the development of this work can reach the following considerations:

- The behavior of the hydraulic power circuit, that is, flow and pressure depend directly on the operation of mechanical devices of the valves responsible for its control. Therefore, the operating characteristics of hydraulic components must be considered during the design of a hydraulic system;
- The delay in the response of the relief valve checked the result without the accumulator was greater with increasing flow variation through this. In a system that operates at high flows this phenomenon could be enlarged due shutter operation of the relief valve, which could bring damage to circuit components;

- The results showed that the accumulator pressure variations become smoother supply acting as a buffer and avoiding too much pressure peaks. It was also found that the variation reduction of supply made by the accumulator was greater in the most critical, ie, at times of high flow variation promoted by VDP cases;
- The results for the variation of pressure do not correspond to those found in real applications because it used components with low flow capacity;
- For future work is suggested to conduct similar experiments done in this work, however using control valves and power unit with capabilities similar to the values commonly used in industrial applications.

REFERENCES

[1] I. V. Linsingen. Fundamentos de Sistemas Hidráulicos. Florianópolis: Editora da UFSC, 2008. 386p.
[2] K. Dasgupta and R. Karmakar. Modelling and Dynamics of Single-Stage Pressure Relief Valve with Directional Damping. Simulation Modelling Practice and Theory – ELSEVIER, Vol. 10, pp. 51-67. 2002.
[3] C. Schwartz. Modeling and Analysis of a Stroke End Cushioning Device for Hydraulic Cylinders, (In Portuguese), M.Sc. Thesis, Universidade Federal de Santa Catarina, Florianopolis, S.C., Brazil, 2004. 110p.
[4] P. I. I. Pereira. Análise Teórico-Experimental de Controladores para Sistemas Hidráulicos. Dissertação de Mestrado, UFSC - Universidade Federal de Santa Catarina, Florianópolis, 2006. 163p.
[5] V. J. de Negri. Sistemas Hidráulicos e Pneumáticos para Automação e Controle – Parte III. Florianópolis: Universidade Federal de Santa Catarina, 2002 (apostila do curso de pós-graduação).
[6] H. L. Stewart. Hydraulic and Pneumatic for Production. New York: Industrial Press. 1977. 435p.
[7] Anthony. E. Fluid Power with Applications. 4 th ed. Ohio: Prentice Hall. 1997. 452p.
[8] R. Szpak. Análise Teórico-Experimental das Pressões em Posicionadores Hidráulicos. Dissertação de Mestrado, UFSC – Universidade Federal de Santa Catarina, Florianópolis, 2008. 132p.
[9] J. Watton. Fundamentals of Fluid Power Control. New York: Cambridge University Press. 2009. 489 p.
[10] M. G. Rabie. Fluid Power Engineering. 1º ed. New York: Editora McGraw-Hill. 2009. 448p.
[11] S. Rao. Vibrações Mecânicas, São Paulo. Ed. Pearson Prentice Hall, 2008. 424p.

EXPERIMENTAL RESEARCH ON VISCOUS FLUID FLOW THROUGH SEALING LABYRINTHS

Lecturer PhD. Eng. Sanda BUDEA[1], PhD.St. Eng. Stefan SIMIONESCU[2], Professor emeritus PhD. Eng. Mircea D. CAZACU[3]

[1] University Politehnica Bucharest, Faculty of Power Engineering, Hydraulics, Hydraulic Machines and Environmental Engineering Department, s_budea@yahoo.com

[2] University Politehnica Bucharest, Faculty of Power Engineering, Hydraulics, Hydraulic Machines and Environmental Engineering Department, stefan_simionescu@yahoo.com

[3] University Politehnica Bucharest, Faculty of Power Engineering, Hydraulics, Hydraulic Machines and Environmental Engineering Department

Abstract: *This article refers to the results of experimental research regarding the viscous fluid flow through sealing labyrinths of turbo machines. This labyrinths can be met both at the interstice between rotor and housing, and in the zone of the interstice of the balancing disc.*
Within the experimental researches, fluid flows through the labyrinths at different Reynolds numbers were visualized, pressure variations along the length of the labyrinth and increase in rotation speed of the mobile ring were analysed. The experimental results have largely overlapped the numerical ones, confirming that the best geometry for the labyrinth with baffles is the one with equal sizes for the channel's depth and width.

Keywords*: labyrinths, baffles, viscous flow, turbo machine.*

1. Introduction

Experimental researches complete the numerical analysis of viscous fluid flow through sealing labyrinths, treated in article [1]. This research aims the knowledge of the flow particularities through different forms of labyrinths in order to establish the conditions that interest the mathematical solving of the problem [7]. The experiments were conducted in a facility specially built for the study of laminar movement of liquids, in the Hydraulic Machinery laboratory of the University Politehnica Bucharest.
The experimental stand operates with oils of different viscosities in order to obtain hydro dynamically similar flows after the Reynolds criterion with geometrically larger models of labyrinths, $\delta/\delta' = 100/1000$, for the ease in visualizing the spectra.

2. Experimentally obtained hydrodynamic spectra

Some hydrodynamic spectra of the actual flow of a real liquid through the straight labyrinth (Fig. 1, a) were presented for illustration, for Reynolds numbers between 3 and 35, and through the baffled labyrinth for Re = 15 (Fig. 1, b) and Re = 20 (fig. 1 c).
On this occasion the following characteristics were observed:

- for these flow regimes, vortical cores do not appear at the labyrinths inlets, due to the stabilization phenomenon of the laminar motion, which translates into an additional local pressure loss;
- the occurrence of vortical cores in the baffled labyrinths allows to assess the dependence of sealing effectiveness on the movement regime, depending on the geometry of the labyrinth and flow configuration;
- the only criterion of effectiveness in a labyrinth seal is represented by a configuration as complex as possible of the stream lines and the possibility of vortex formation in certain areas, convenient for a higher braking of the flow.

Since in this flow phenomenon, an important role is played by the rotation velocity of the labyrinth's mobile ring, we designed and realized a variant of a special facility for the investigation of the flow through the labyrinth in real conditions. This facility can work with pressures and peripheral velocities up to the highest permitted in modern design of turbo machinery, due to the hydraulic balancing of the axial force and the stiffening of the shaft.

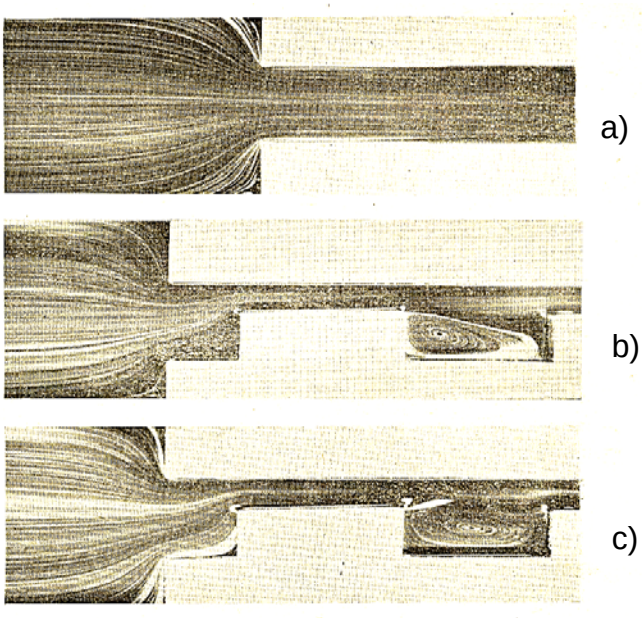

Fig. 1. Hydrodynamic spectra of the 2D movement through the straight labyrinth without and with baffles, as obtained in the facility for the study of viscous fluid flow at a) Re=3…35; b) Re=15; c) Re=20

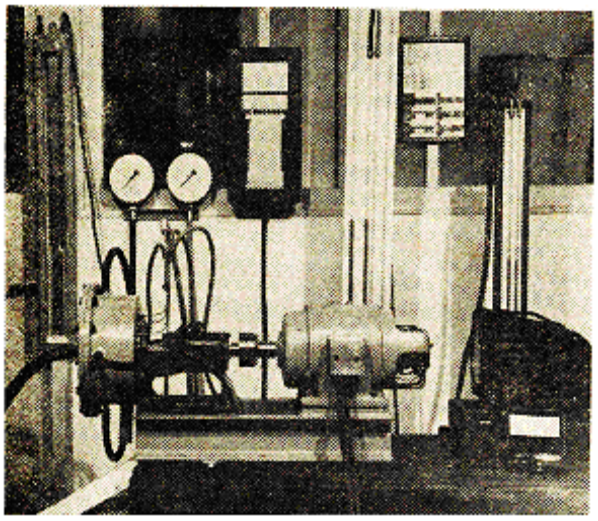

Fig. 2.The stand for experimental tests [6]

The experimental stand allows simultaneous study of two sealing labyrinths of different shapes (Fig. 2).
The pressure in the system was carried out by a multistage centrifugal pump. Pressure plugs were practiced in the fixed ring of the labyrinth, for a good knowledge of the pressure distribution along the labyrinth.
Due to the relatively small sizes of the labyrinths, a particular attention was given to respecting their shape and size, surface quality, and the outer ring and inner balance.

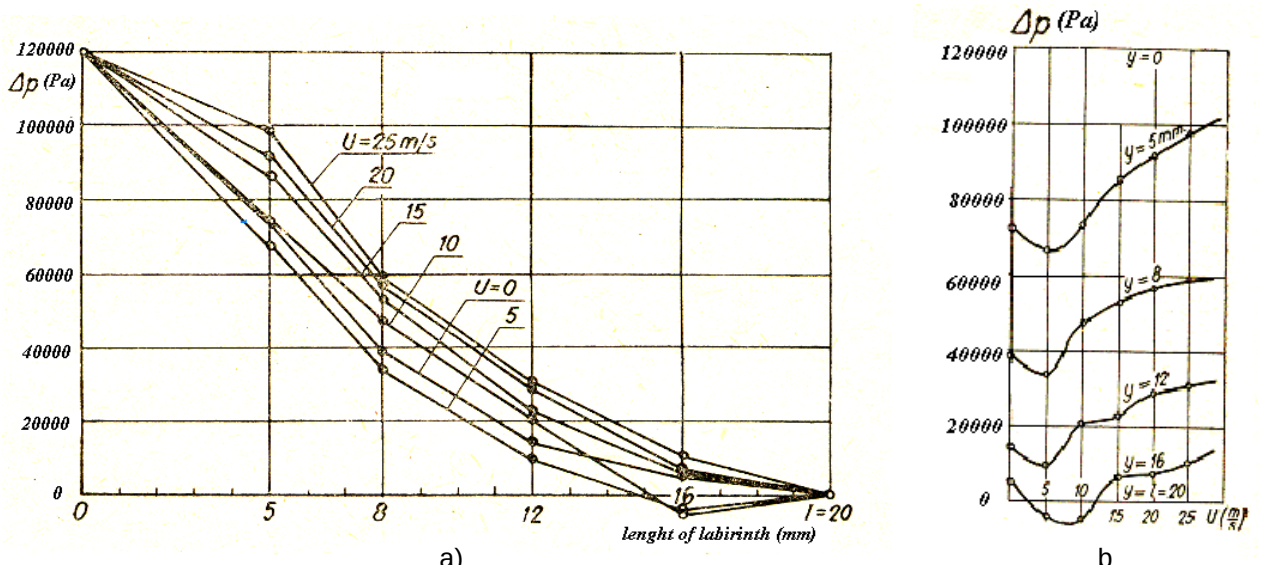

Fig. 3. Pressure variation: a) along the labyrinth; b) at different rotation velocities of the mobile ring [6]

In Figure 3 a) is shown the variation of pressure along the labyrinth l (mm), and Figure 3 b) shows the variation of pressure at different rotational velocities U (m/s), results from tests made with water. These studies have revealed the influence of the rotation velocity of the labyrinth's mobile ring on its sealing capacity.
The minimum sealing capacity occurs approximately at the value of 1 of the rotational velocities coefficient [6], which is a general phenomenon in the theory of hydrodynamic similarity, and which corresponds to a qualitative change of the movement.

3. Comparative analysis: CFD and experiments

From a comparative analysis of pressure variations resulting from numerical simulation and those obtained experimentally, values represented in Figure 4, one can see the intersection of values for most of the labyrinth's length, with values slightly different at the inlet and outlet of the labyrinth. We obtained stable numerical solutions at low rotation velocities (0.5 or 10 m/s). This values clearly overlapping on the values obtained experimentally.

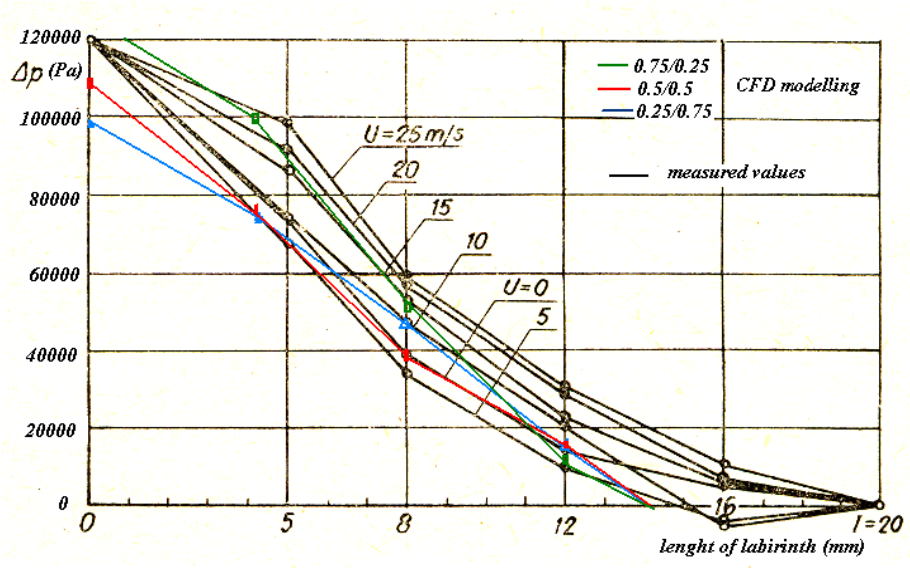

Fig. 4 Numerical and experimental results for fluid flow through turbo machines labyrinths

This comparison also revealed that the greatest areas overlap was found for the labyrinth with the geometric ratio 0.5 / 0.5, i.e. equal values of the depth, width and stepof the baffles.

4. Conclusions

Numerical modelling of a viscous fluid flow through turbo machines labyrinths led to the following observations: the flow velocities varies between the inlet and outlet of the labyrinth in all three geometries studied; as the depth of labyrinth's baffle increased, velocities were reduced along the labyrinth; approximate equal values of velocity were registered for a depth of the channel equal to the width (in parametric design 0.5/0.5). This together with the 0.4/0.6 depth to width ratio design would represent the optimal configurations of the labyrinths.
The pressure drop along the labyrinth was different, more rapid at deeper baffles. Stream lines spectrum revealed formation of vortices in the flow in the area of labyrinth baffles, as the viscous fluid flow passes through them, providing the labyrinth sealing. Stable numerical solutions were obtained for small rotational velocities (0, 5 or 10 m/s).
In the experimental research flows at different Reynolds numbers were visualized, pressure variations along the length of the labyrinth were analysed and the increase in rotational velocity of the mobile ring. The numerical results overlapped largely over the experimental ones.
These observations led us to conclude that an optimal labyrinth with baffles has the depth of baffles at most equal to the width of the channel of flow in the labyrinth, and the step of baffles equal to this depth.
Similar numerical and experimental approaches were identified in articles [2-5].
This research will be extended by further investigations regarding the effect of geometry on the increase in hydraulic efficiency of turbo machines.

REFERENCES

[1] S. Budea, St. Simionescu, "Numerical modeling of viscous fluid flow by sealing labyrinths", Hidraulica Magazine, No. 1 /2014, ISSN 1453-7303;
[2] Rhode, DL; Morrison, GL - "Experimental and numerical assessment of an advanced labyrinth seal", *Tribology transactions* 37(4), 743-750, 2008;
[3] Kirk R.G., Guo Z.,"Influence of Leak Path Friction on Labyrinth Seal Inlet Swirl", *Tribology transactions* 52(2), 139-145, 2009;
[4] Liu, Z.P.; Liu, S. L., Zheng, S.Y., "A New Numerical Method to Realize Unsteady Calculation of Flow in Labyrinth Seals",*Advances in Mechanical Design*, PTS 1 AND 2Book Series: Advanced Materials Research Volume: 199-200, 68-71, 2011;
[5] Hirono T., Guo Z.L., Kirk R.G., „Application of computational fluid dynamics analysus for rotating machinery – Part II: Labyrinth seal analysis", *Journal of engineering for gas turbines and power transaction of the ASME*, Vol 127 (4), 820-826, 2005;
[6] Cazacu M.D., Budea S.,„Curgeri tridimensionale ale fluidelor vascoase prin masini si echipamente", Editura Printech, 2012, 92-112;
[7] Cazacu M.D.,„On the boundary conditions in three-dimensional viscos flow", The 5th Congres of Romanian Matematicians, June 22-28, 24-26, 2003.

MECHATRONIC DRIVE SYSTEM FOR CLEANING MACHINE OF PHOTOVOLTAIC PANELS

PhD. eng. Radu RADOI[1], PhD. eng. Marian BLEJAN[1], PhD. St. eng. Ioana ILIE[1]

[1] INOE 2000 - IHP, radoi.ihp@fluidas.ro
blejan.ihp@fluidas.ro
ilie.ihp@fluidas.ro

Abstract: *The efficiency of the photovoltaic panels depend on the cleanliness of the reception surface of solar energy. As in time on this are deposited all kinds of impurities, the productive efficiency can drop even up to 50 %. It is necessary from this cause their regular cleaning. The paper presents the structure of the cleaning machine, hydraulic scheme and the mechatronic system based on a unit with microcontroller.*

Keywords*: mechatronic drive system, pv washing, controller*

1. Introduction

The efficiency of the photovoltaic panels depend on the cleanliness of the reception surface of solar energy. As in time on this are deposited all kinds of impurities, the productive efficiency can drop even up to 50 %. It is necessary from this cause their regular cleaning. For this was developed a cleaning machine which required a mechatronic drive system to control his functioning.

Comparison between systems

	Cleaning Systems					
	1. Manual	**2.Water jet**	**3.With compressed air jet**	**4.With steam jet**	**5. With sprinklers**	**6. With sliding brush**
Efficiency	80 – 90%	70 – 80%	70%	90%	70%	70%
Cost/kWh	high	average-high	average	scăzut	mediu	average
Water consumption	6,5÷12% l/m^2	2,5 ÷ 2,8 l/m^2	-	0,5÷ 0,6 l/m	6,5÷12 l/m^2	-
Labor	4÷5 m^2/min with 4 operators	18–20 m^2/min with 3 operators	15-20 m^2/min with 3 operators	22-27 m^2/min with 1 operator	-	-

2. The structure of the cleaning machine for photovoltaic panels

The cleaning machine (Figure 1, 6) combines washing system with low pressure water jet (~2 bar) with brushing the photovoltaic panel. The mechanics and kinematics of the machine was developed by the R&D institute ICTCM Bucharest, and mechatronic drive system for hydraulic installation was developed by the R&D institute INOE 2000 – IHP Bucharest. Mechanics of the cleaning machine and related peripheral systems are loaded on a Toyota Hilux utility vehicle. The mechanism incorporates a 180° rotatable pivot driven by a toothed rack - gear wheel type mechanism.The toothed rack is driven left or right by a hydraulic cylinder. At the upper end of the pivot is mounted an arm that has at end a swivel support that is driven through some levers by the hydraulic cylinder **(14)**. Inclination of the arm is made with the hydraulic cylinder **(2)**. Rotating of the brush is provided by hydraulic motor **(32).** On the brush holder are mounted nozzles that

provide washing of the PV with waterjet. The hydraulic cylinder **(2)** performs vertical positioning of the brush to the photovoltaic panel and the hydraulic cylinder **(14)** performs positioning of the brush parallel to the panel. These cylinders must constantly correct vertical position of the brush and angular position because of irregularities of mounting of the panels and due to the irregularities of the terrain encountered on the route conducted by car along of the panels.
On the same utility vehicle is loaded water pump hydraulically driven, hydraulic station for driving hydraulic motors, the combustion engine which act the hydraulic pumps and the water tank for washing.

The heat engine that provides energy for hydraulic station is a 4.5 kW diesel engine with 2200 rev / min.

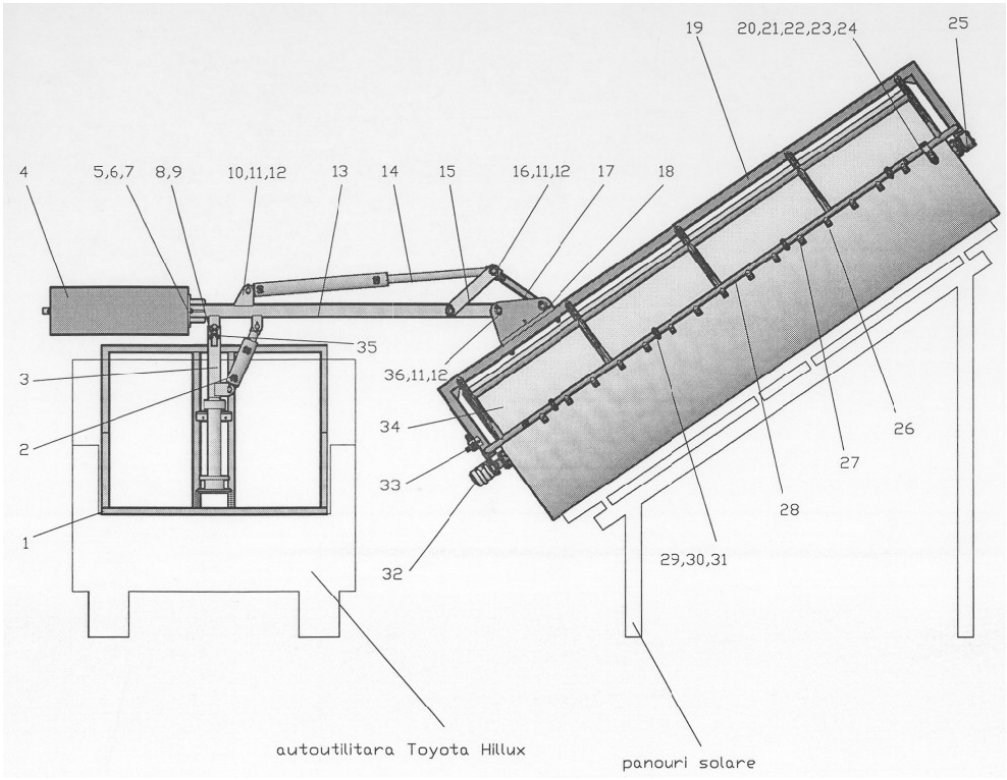

Figure 1

3. Hydraulic drive scheme

Hydraulic station of which diagram is shown in the figure 2 is composed of:

- Hydraulic tank of 100 l with return filter and oil cooling system. Solenoid valve **(20.2)** turns on or off, depending on the command received from a thermostat, the coolant. Washing water circuit is used as a coolant.
- Pumping group comprising a triple pump driven by a combustion engine of 4.5 kW. The first section of the pumping unit has parameters of 14 l / min and 100 bar feed a pressure bus of which with hydraulic directional valves **10.1, 10.2** and **10.3** are supplied hydraulic cylinders **17,18** and **19** providing vertical positioning of the brush, angular motion or rotating the pivot.

The second section of the pumping group with parameters 4.5 l / min and 60 bar, act through the directional valve **(11)** the hydraulic motor for rotating the brush in direction left or direction right with speed of 125 rev / min.

The third pumping section with parameters 7,5 l/min and 50 bar, act through directional valve **(12** the hydraulic motor for water pump at a speed of 2800 rev / min.

The pressure line for the first pumping section is provided with a hydropneumatic accumulator which is designed to store a volume of about 0.3 l of oil at the stages when its consumers do not consume oil and to restore in the system when its consumers are activated.

A loop of automation based on signals from pressure switches 9.1 and 9.2 download to tank the first pumping section when pressure reaches 120 bar and connect back to the pressure line when the pressure dropped to 90 bar with directional valve (6).

For accidental situation when heat engine is defective in work field, to execute movements for folding the mechanism in the marching position of the vehicle, was set a hydraulic electric pump (26) with parameters of 500 W, 2.5 l / min and 100 bar, supplied from the vehicle's electrical system (12 V).

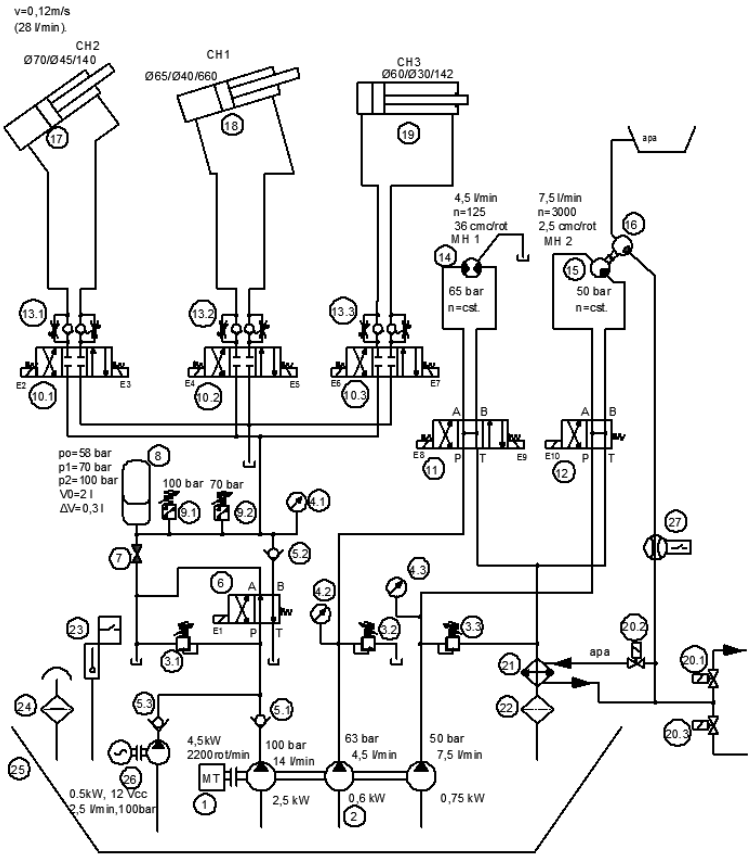

Figure 2

4. The mechatronic system

Automating of the installation is based on a microcontroller unit that receives information from sensors, from contacts limiter, thermostat and the pressure switches and gives commands to the valves coils for making various movements. Electrical commands are given through high side switches IC's. Commands received by the valves enable a mechanisms movements such as rotating column, arm tilt, brush angle adjustment and controlling valves for washing on the left side, on the right side or cooling circuit. To keep the brush distance from solar panels was implemented a control loop with two ultrasonic distance transducers. The average distance given by the distance transducers from the ends of the brush constitutes the command for positioning the height of brush through the directional valve for arm tilt (Figure 3).The difference of the distances given by transducers on the ends of the brush constitutes the command to directional valve for brush angle, in order to keep distance from the brush to the solar panel. In the figure 4 can be seen the box with controller module, and in figure 5 the remote control unit which permit to the operator to control the cleaning installation.

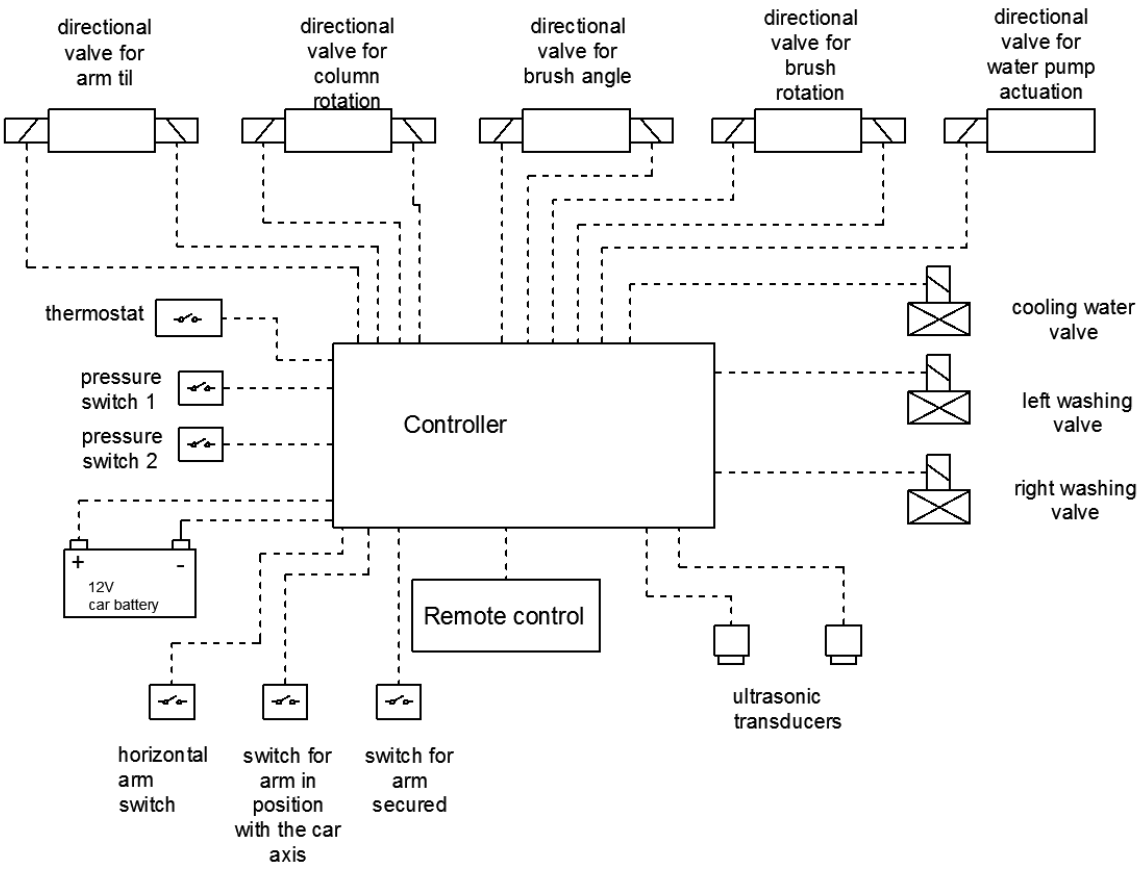

Figure 3

Figure 4

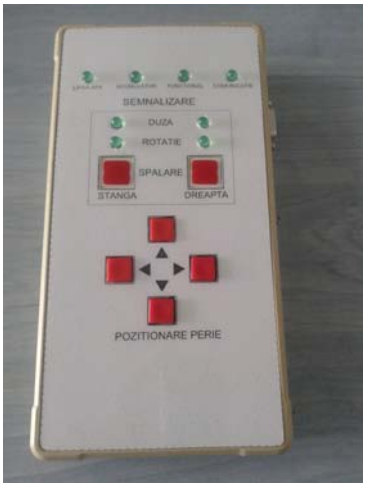

Figure 5

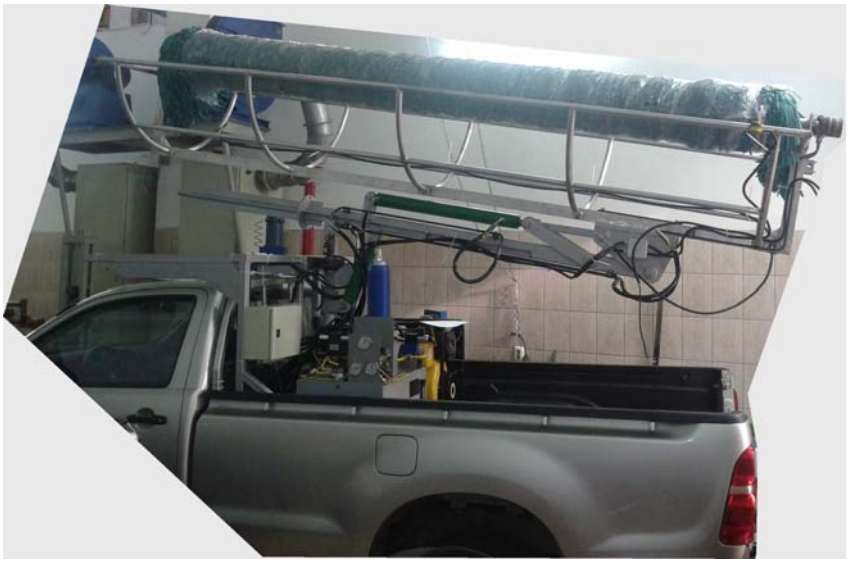

Figure 6

5. Conclusions

The project is very complex and required design in terms of kinematics, hydraulics and mechatronic systems.
The washing machine for solar photovoltaic panels is the first of its kind being developed in the country and is in prototype stage.
Experiments are underway to carry out adjustments and determine technical performances.

REFERENCES

[1] Sami Al-Ghannam, Comparison Analysis on Different Cleaning Technologies for Photovoltaic Panels of Utility Scale Application, Saudi Aramco Study pdf, 2012
V. Marin, R. Moscovici, D. Teneslav, Sisteme hidraulice de reglare automată – Probleme practice, Editura Tehnică Bucureşti, 1981
[2] G. Rădulescu, R. Rădoi, I.Duţu, Complex systems for electrohydraulic drive mechatronic, Caciulata, Romania; 7-9 November, 2009, "Proceedings - HERVEX", ISSN 1454-8003; pp.182-187
[3] http://www.solar-facts-and-advice.com/solar-panel-cleaning.html
[4] http://www.ipceagle.com/products/solar-panel-pure-water-cleaning-system#.VEeGzhbHRjU
[5] http://www.bitimec.com/bitimec_page.asp?IDProdotto=315
[6] http://www.saudi-sg.com/2012/files/B42.pdf

INFLUENCE OF NITRIDING THERMOCHEMICAL TREATMENTS UPON CAVITATION EROSION RESISTANCE OF DUPLEX X2CrNiMoN22-5-3 STAINLESS STEELS

Assist. PhD.eng. Lavinia Madalina MICU[1], Student Dorin BORDEASU[2], Prof. PhD.eng. Ilare BORDEASU[3], Assoc. Prof. PhD.eng. Mihaela POPESCU[4], PhD.eng. Octavian Victor OANCA[5], Lecturer PhD.eng. Sebastian Titus DUMA[6]

[1] Politehnica University of Timisoara, lavimicu@yahoo.com

[2] Via University College, Horsens, Denmark, dorin_craiova@yahoo.com

[3]Politehnica University of Timisoara, ilarica59@gmail.com

[4]Politehnica University of Timisoara, hela.popescu@yahoo.com

[5]Politehnica University of Timisoara, octavian.oanca@yahoo.com

[6]Politehnica University of Timisoara, sduma_titus@yahoo.com

Abstract: *The duplex stainless steels X2CrNiMoN22-5-3 is widely used today, in chemical industry, in shipbuilding industry, in construction industry, in food industry etc., because it has good resistance to intercrystalline corrosion and, better physical and mechanical properties then austenitic steels. The mechanical properties of those steels, depends very much on their chemical composition and on the applied treatment. This paper presents the effect and the advantage of applying nitrogen during the nitriding thermochemical process upon the cavitation erosion resistance of the stainless steels X2CrNiMoN22-5-3, in comparison with the quenching heat treatment and low tempering. The researches were undertaken at Timisoara "Politehnica" University in the Cavitation Laboratory, using a piezoelectric crystal vibratory device T2. By comparing the interpretation of the specific curves M(t) and v(t) (cumulative mass losses and erosion rate) of the two analyzed treatment procedures (one of gas nitriding (ammonia), and the second of quenching and oven cooling) with the ones of standard steel OH12NDL, utilized in Kaplan turbine blades used in Romania, in the hydropower called "Portile de fier", results in a significant increase of the resistance against the vibratory cavitation erosion. Also, it is observed and certified that gas nitriding treatment, gives to stainless steel X2CrNiMoN22-5-3 a higher cavitation resistance then the one resulting from quenching heat treatment. Therefore, the test results shows that, the type of treatment applied to stainless steel X2CrNiMoN22-5-3, influence the increase of the exposed surface to cavitation erosion resistance.*

Keywords*: duplex stainless steel, gas nitriding, quenching and oven cooling, cavitation resistance, the mean depth erosion, erosion rate, cumulative mass losses*

1. Introduction

Destroying the solid materials through cavitation, represents a complex phenomenon, involving a hydrodynamic and mechanical aspect according to their material fatigue life. [1], [2]. The research done until now, in cavitation erosion domain, were aimed to identify the most resistant materials needed to manufacture steam turbine blades, ship propellers, missiles, hydraulic machinery rotors etc. While today, its focusing on studying the solid material behavior at different cavitation stages, and on the metallographic study, a study based on microphotography obtained optically or electronically [3], [4], [5], [7]

In general, the duplex stainless steel presents better mechanical and errosion resistance properties then austenitic ones, but those properties depends on the chemical composition and the applied treatment [6], [8], [9].

By applying the cooling quenching and oven cooling heat treatment to the duplex stainless steel X2CrNiMoN22-5-3, the good mechanical properties (tensile strength, hardness, yield point) are ensured, and the chromium presence of chromium in δ ferrite structure gives a good resistance to intercrystalline corrosion.
By applying gas (ammonia) nitriding thermochemical treatment, the austenitic-ferrite stainless steel, X2CrNiMoN22-5-3, was aimed to achieve a superficial hardness, and a good resistance to fatigue and to cavitation erosion.
Taking into account the research done until now, regarding different ways for increasing the stainless steels cavitation erosion resistance, the present work highlights the effect of the thermochemical treatment applied to the duplex stainless steel compared to the volumic heat treatments regarding the increase in resistance to cavitation attack.
The analysis of the two types of treatments applied to stainless steel X2CrNiMoN22-5-3, was done by comparison with the characteristics of the standard steel - OH12NDL known by all hydraulic turbines manufacturers in Romania, as having very good resistance to cavitation erosion.

2. Researched material. Devices and research method

The researched material are duplex stainless steel, symbolized X2CrNiMoN22-5-3 [6] and standard stainless steel, with primarily martensitic structure, OH12NDL [6].
In the first table, are given the micro hardness HV values, measured on the surface of the specimens, taken from the duplex and the standard steel, which were exposed to the cavitation attack.

Table 1. Micro hardeness, researched in specified states [1], [14]

Steel Symbolisation	**Hardness HV1**
X2CrNiMoN22-5-3 – recieved state	252
X2CrNiMoN22-5-3 – gas nitiriding state	651
X2CrNiMoN22-5-3 – quenched and oven cooled, state	275
OH12NDL-samples from the spare blades of Kaplan rotor from CHE "Portile de Fier I"	237

According to Table 1 data, Duplex stainless steel, X2CrNiMoN22-5-3, in nitrided state shows the highest micro hardness value compared to other states of the same steel (around 2.6 times higher than the delivered one, and around 2.6 higher than the quenched one), and compared to the standard one (around 2.7 times higher). Considering that this increase is due to nitrogen increase into the surface, results the formation of finely dispersed chromium nitride precipitates [12].
For both steels, were made specimens, that were exposed to cavitational erosion, for 165 minutes, in drinking water of the public grid, at 20-22°C, according to ASTM G 32-2010 standards, regarding the functional parameters of the standar piezoceramic crystal device T2 standard and the standard research procedure [3], [6], [10].
The vibrator device, Figure 1, used in cavitation generation, its owned by Timisoara "Politehnica" University in the Cavitation Laboratory.
Regarding the experiment development procedure, the specimen is mounted on the sonotrode, and immersed up to the squeezing cavity in drinking water, at a temperature of 20-22 ° C, followed by the cavitation test, for a given time (the total duration was 165 minutes divided into 5 minute period (one), 10 minutes (one) and the rest 10 periods, 15 minutes each one). After the cavitation test, the specimen is washed in water and then in acetone. Before weighting the specimen was dried with hot air. The eroded mass is measured with Za₮klady Mechaniki Precyzyjnej WP 1 analytical scale, which has an accuracy of 10^{-5} grams.
For comparison, the evolution of the surface degradation development under the shock waves impact and the cavitation bubble implosion generated by the microjets, in fig. 2 is given the 90th minute picture of the cavitation attack, and in fig. 3 the picture at the end of the attack.
Because, at the end of the cavitation attack, the samples were analyzed with optical microscope, for highlighting the damage shape, in fig. 3 is presented also the axial splitting procedure (into two

halves), on the diameter ,chosen arbitrarily fixed in resin, and measuring the deepest depths. The parts secured in resin were polished before being microscopically analyzed.

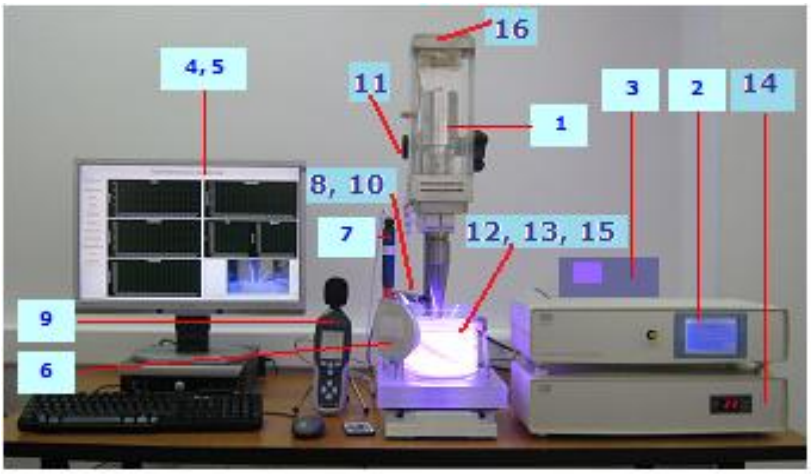

Fig. 1 T2 piezoceramic crystal device
(1. mechanical resonator assembly (20 kHz +/- 200 Hz); 2. ultrasonic generator (240V/50Hz, 20kHz, 500W); 3. PLC data acquisition interface; 4. DELL OPTIPLEX 745 operating system; 5. LCD Monitor PHILIPS; 6. PLANET networking System HD; 7. ProMinent pH-meter; 8. infrared temperature sensor OMEGA Enginnering.Inc; 9. Sound Meter SL-451 VOLTCRAFT; 10. temperature sensor; 11. Mechanical resonator assembly support; 12. Cavitational liquid Flask; 13. Cooling system liquid; 14. Circulation and filtration system for cooling liquid; 15. Flask lightnening system 16. Mechanical resonator assembly ventilation system)

The cavitational experiment was done on three sets of samples: two sets of Duplex stainless steel type X2CrNiMoN22-5-3 and one set of standard steel - OH12NDL.
According to ASTM G32-2010, each set of samples contained three samples.
The first investigated set of steel specimens, was X2CrNiMoN22-5-3, containing the specimens heat treated by quenching at a temperature of 1060 ° C for 30 minutes, followed by oven cooling. The second set of steel specimens, was the one treated thermochemical in nitriding gas environment (at a temperature of 520 ° C, in ammonia). The heat treatment was done in Timisoara "Politehnica" University, in the Laboratory of Materials Science, and the thermochemical one was done in S.C. Duroterm S.A. Bucharest.

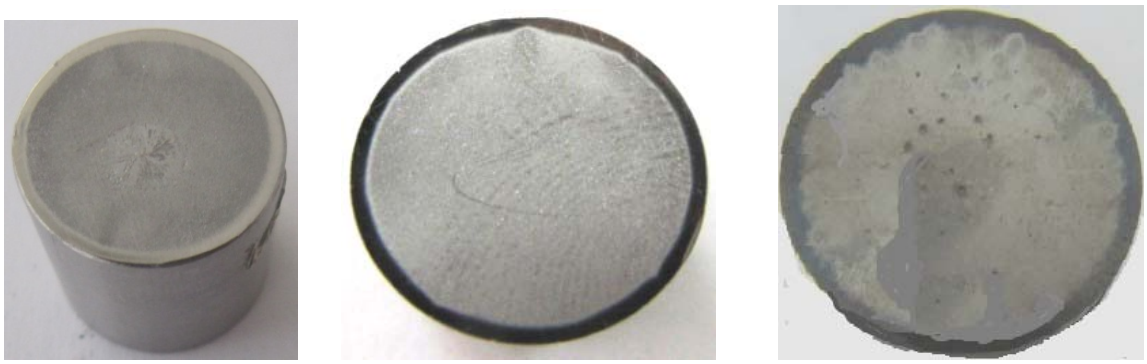

a. Standard (OH12NDL) b. Quenched c. Nitrided in gas

Fig.2 Pictures from 90th minute of surfaces exposed to cavitational attack

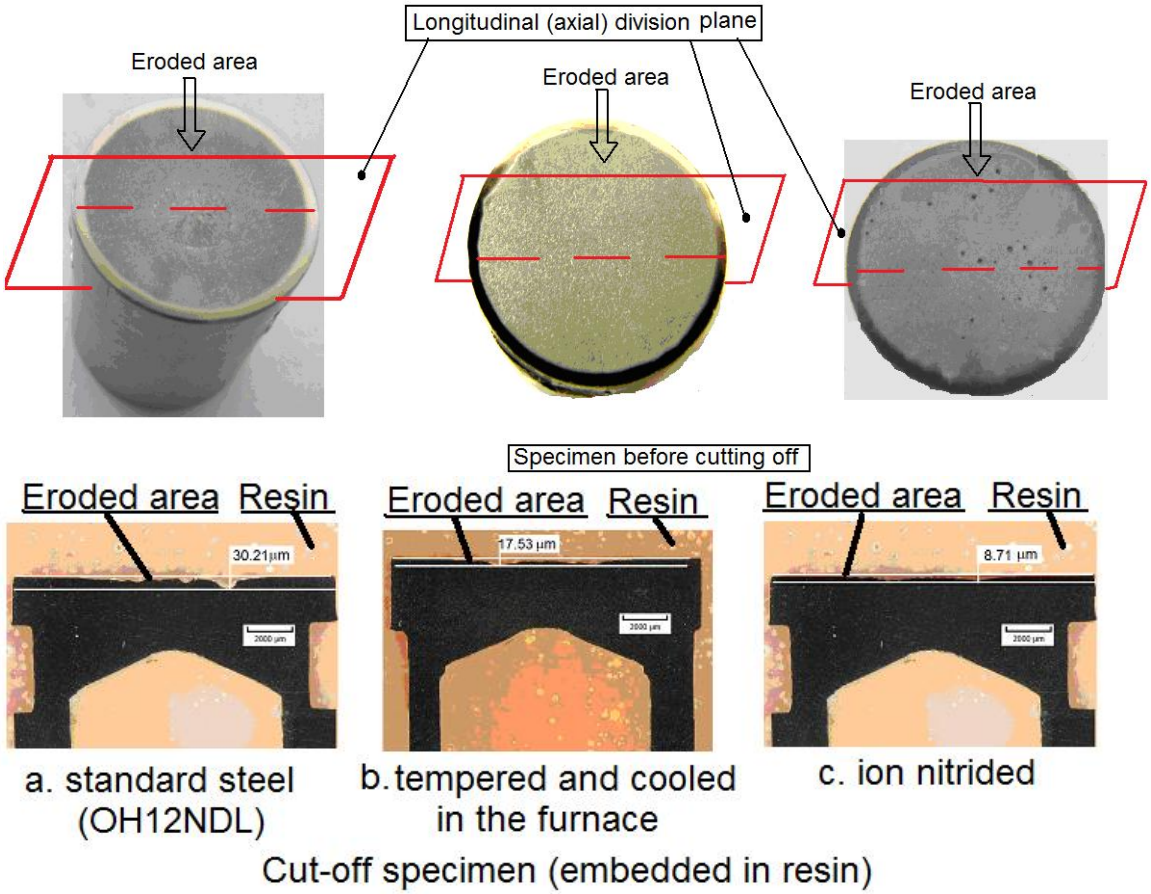

Fig.3 Pictures of the eroded surfaces after 165 minutes of cavitation test (Specimens preparation for microscopic analyze)

From Figure 3, the pictures with the specimens secured in resin, it can be observed that the penetration depth of the specimens heat-treated (17,53 μm) and thermochemical treated (8,71 μm) are significantly lower than the one resulting from the standard steel specimen (30,21 μm), which shows the beneficial effect of the treatment regarding the cavitation resistance.

3. Experimental results

In figure 4, are presented the specific erosion curves, constructed based on cumulative mass losses, obtained after weighting the cavitated specimens. As it can be seen, the nitrided specimens, presents a greater resistance to cavitation erosion, therefore the losses were much lower during the entire period of attack. This happens, mainly, due to steel hardness obtained after being nitriding treated in the gas.
According to figure 4 diagram, the most mass losses at the end of cavitation erosion test, were obtained for the standard steel OH12NDL, followed by stainless steel Duplex (X2CrNiMoN22-5-3) heat treated by quenching. These results confirms that by applying a single heat treatment, quenching, the steel cavitation erosion resistance increase; because by quenching acquires a martensitic structure on deep area, having a higher hardness and a better cavitation resistance.

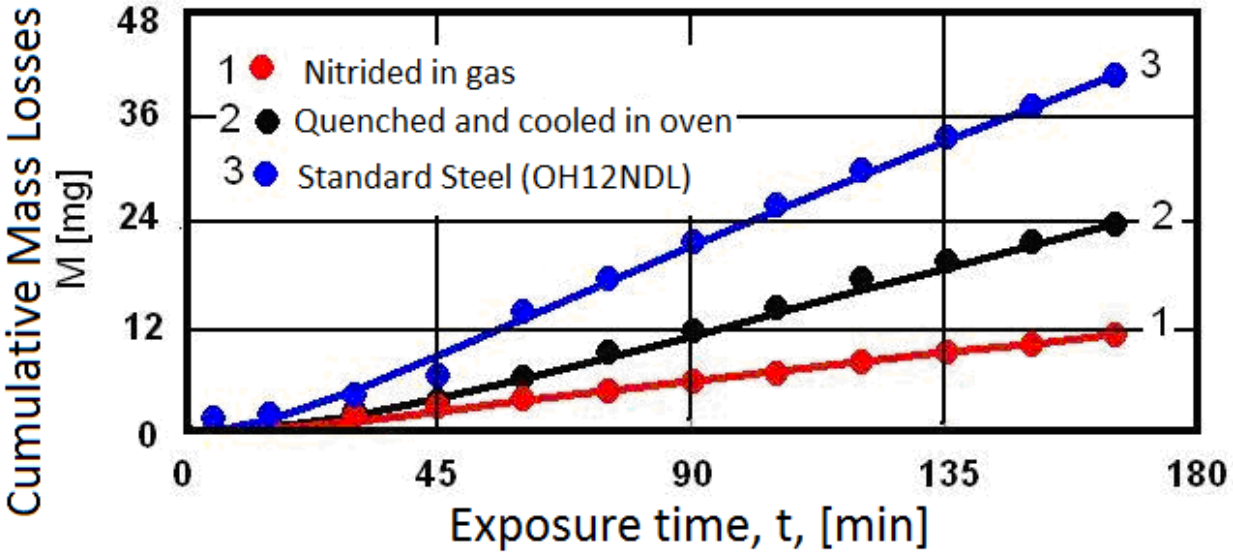

Fig.4. (Cumulative) Weight losses variation according to exposure time

From the losses recorded at the end of 165 minutes, results that, related to the standard steel, the duplex steel X2CrNiMoN22-5-3 diminish its weight lost through erosion with almost 41.7% by quenching with air cooling, and with almost 73,5 % by gas nitriding (ammonia). Also it can be observed the thermochemical treatment provides superiority compare to the thermal one because the mass losses decreased with almost 54.5%.
Figure 5 presents the evolution of erosion rate curves of Duplex stainless steel, the two states, compared with the standard steel OH12NDL.

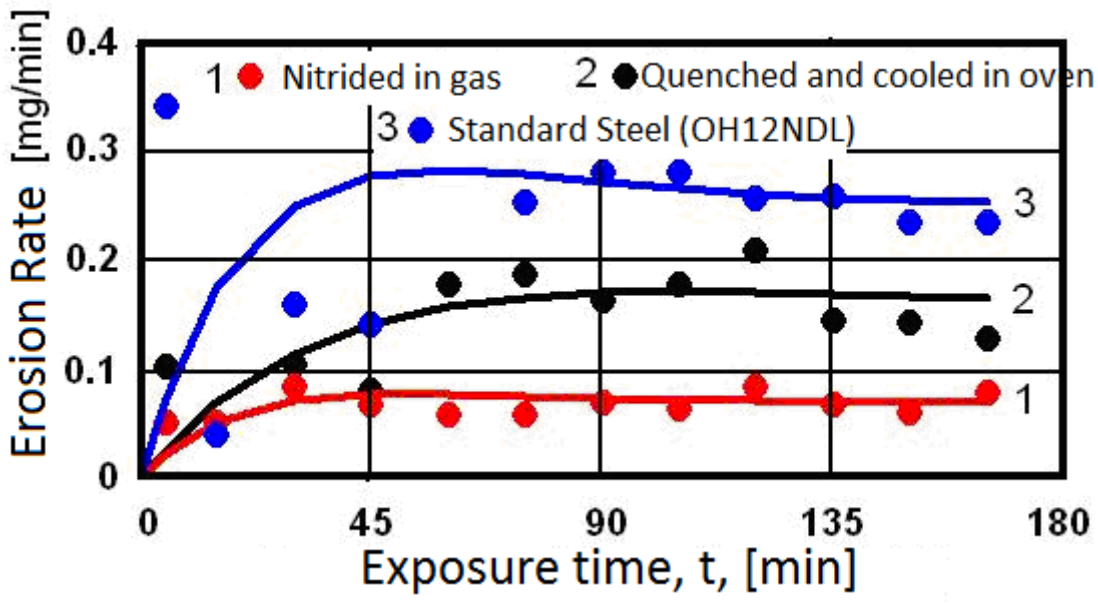

Fig.5. Erosion rate according to the exposure time

It was found that, by applying nitriding thermochemical treatment, the stainless steel X2CrNiMoN22-5-3 was recording a significant decrease of the erosion rate, created by micro jets in the body, (around 0,24 mg/min) compared with the same steel heat treated by quenching (around 0,066 mg/min), but both of them record a lower decrease then the standard steel (around 0,164 mg/min).

Regarding the resistance increase, taking as reference the value to which the speed tends to stabilize (fig.5), results that by gas nitriding, the researched duplex steel increases its resistance to cavitation with around 60 % compared to the state obtained by quenched and cooled in the oven, and approximately 72,5% compared to the standard steel.
During the same time, it can be also seen the quenching and oven cooling effect, resulting in a large increase of the cavitation erosion resistance. Compared to standard steel, the erosion rate increases with almost 32 %.
Therefore both treatments are advisable to be used, especially where duplex steel X2CrNiMoN22-5-3 is used to manufacture the parts used in cavitation.
In the fig.6 diagram are compared, the mean depths of erosion, resulted by approximating the data points from fig. 4, with the maximum values measured in the axial sections fig.3.

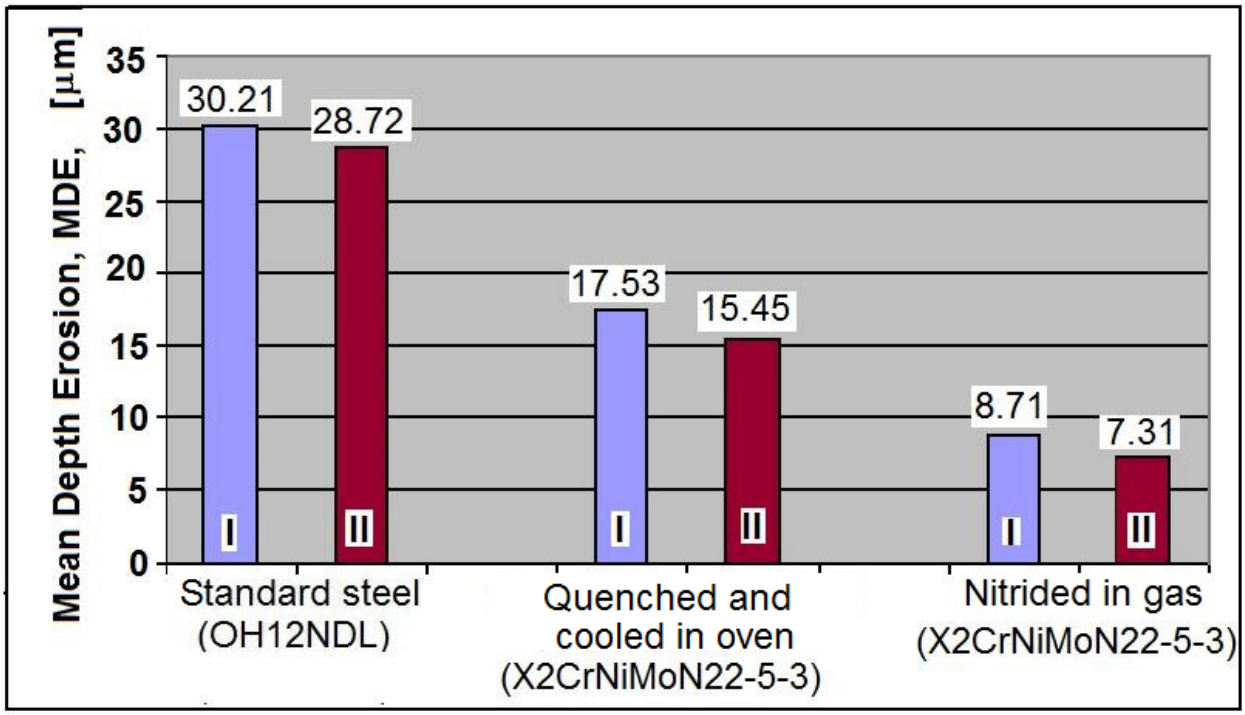

Fig. 6 Mean Depth Erosion
I – Maximum measured value in the cut – off section performed according to fig.3
II – Average of the cumulative mass losses at the end of cavitation attack (fig.4)

From fig. 6 it can be distinguished, the differences between the depths resulted from the cumulated mass losses and the measured ones, in an arbitrary cut-off section, as the one presented in fig.3. These differences are natural, but not especially in this form, and present that:
- The cavitation erosion is not a uniform process through the entire exposed area, depending on the expelled grain size, structural defects, uniformity of the surface mechanical properties, grain size, etc.
- The cumulative depths presented in fig.4 are average values, obtained by calculation, where the size of the area damaged by cavitation its involved, material density and obviously the measured mass.

4. Conclusions

Important conclusions, regarding the aimed purpose by the results presented in this paper, are given by the comparison of the cavitation resistance of duplex steel X2CrNiMoN22-5-3 in the two states, with the one of the standard steel OH12NDL, a steel considered with good resistance to cavitation.

- Using the gas (ammonia) nitriding thermochemical treatment, on the parts that operates in intense cavitation flow conditions, is recommended, because is giving an increase of hardness which provides a large increase in resistance to cavitation attack.
- Applying the volumic heat treatment, as the quenching with oven cooling, remains the classical method through which the cavitation resistance of duplex stainless steels can be improved.
- Regarding the cavitation resistance improvements of X2CrNiMoN22-5-3 duplex steel, the thermochemical treatment efficiency is higher than the quenching and oven cooling one..

REFERENCES

[1] I. Anton, "Cavitatia", Vol.I, Editura Academiei RSR, 1984
[2] I. Bordeaşu, „Eroziunea cavitaţională a materialelor", Editura Politehnica, Timişoara, 2006;
[3] I. Bordeașu, M.O. Popoviciu, "Improving cavitation erosion resistance through surface and structural hardening", Machine Designe, PP. ISSN ISSN 1821-1259, 2012
[4] I. Bordeaşu, I. Mitelea, "Cavitation Erosion Behavior for some Stainless Steels with Constant Nickel and variable Chromium Content", MP Material Testing, Issue 01, ISSN: 0025-530, pp. 53-58, 2012;
[5] J.P. Frank, J. M. Michel, "Fundamentals of cavitation" Kluwer Academic Publishers-Dordrecht/Boston/London, 2004;
[6] M. L. Micu, I. Bordeaşu, I. Mitelea, C. Ghera, Laura Sălcianu, „Cercetarea eroziunii cavitaţionale asupra oţelului inoxidabil X2CrNiMn22-5-3 tratat termic", Ştiinţă şi Inginerie, an XIV, vol.26/2014, Sebeş – Alba, ISSN: 2067-7138, Editura AGIR, Bucureşti, 2014, p.425-430;
[7] I. Mitelea, „Ştiinţa materialelor", vol.I, Editura Politehnica, ISBN 978-973-625-826-8, 2009;
[8] L. Sălcianu, I. Bordeaşu, M.L. Micu L, M., Cr. Ghera, „Rezistenta la eroziunea cavitatiei a doua oteluri inoxidabile diferite structural si supuse aceluiasi tratament termic volumic", Conferinta Nationala Multidiciplinara „Profesorul Ion D Lazarescu" fondatorul scolii romanesti de teoria aschierii, Editia I Cugir, 2014, pp.675-682 **;**
[9] M. Truşculescu, A. Ieremia, „Oţeluri inoxidabile şi refractare", Editura Facla, Timişoara, 1983;
[10] *** Standard method of vibratory cavitation erosion test, ASTM, Standard G32, 2010;
[11] *** http://www.inoxservice.hu/index.php/ro/rozsdamentesacel;
[12] *** http://ccimn.ulbsibiu.ro/documente/carti/notare_dt.pdf

ACKNOWLEDGMENT: ***This work was partially supported by the strategic grant "Cresterea atractivitatii si performantei programelor de formare doctorala si postdoctorala pentru cercetatori in stiinte ingineresti – ATRACTING", având ca beneficiar Universitatea Politehnica Timisoara, finanțat prin contractul POSDRU/159/1.5/S/137070 2014- 2015***

TRIBOLOGY PERSPECTIVE ON SEATBELT PRETENSIONING SYSTEM

Tribology perspective on seatbelt pretensioning mechanism

Dipl.eng. Paul IMRE[1]

[1] Technical University of Cluj-Napoca, ROMANIA, imrepaul@yahoo.com

Abstract: *This paper presents the factors and forces involved in the concept propulsion unit of a seatbelt pretensioning mechanism. The function and role of seatbelt pretensioning will be presented as an introduction, but the paper will focus on the propulsion from a tribology perspective focusing on the experiments and simulations performed to determine the factors of influence in this system.*

Keywords*: tribology, forces, lubricants, simulations, design of experiment*

1. Introduction

The pretensioning systems for seatbelts are designed to reduce the excess of webbing in the seatbelt system during and crash, this assures for a better fixing of the occupant in the seat, thus reducing the forward movement of the chest and the pelvis area. The system is presented in *figure 1*.

The evolution of pretensioning systems for the seatbelt has its roots in the need of automobile manufactures to constantly increase the performance, reduce the weight and overall size of the parts and also to avoid over engineering of all components used in the vehicle.

Fig.1. Pretensioning role during a car crash [3]

In the following chapters I will present a concept for the propulsion unit, this unit is activated by a gas generator which creates the necessary pressure on the surface of a piston in order to apply enough force on the seatbelt webbing to obtain the webbing excess reduction and improve the occupant positioning.

I will present the analysis performed on the mechanism using tests and simulations to be able to better understand the forces that are involved and improve the system.

2. Mechanism and function description

The pretensioning mechanism that will be discussed in this paper has two functions that can be investigated as individual entities, first we have the module that has to assure the restraint of the seatbelt webbing and it's fixation to either the car body or the seat frame and secondly there is the part that assures the pretensioning function.

In *figure 2* the whole mechanism is presented and the two separate functions as shown above are shown. The focus in this paper will be on the forces and contacts that affect the pretensioning function in order to better understand the main causes for loosing energy in the system and to be able to further develop and improve the product.

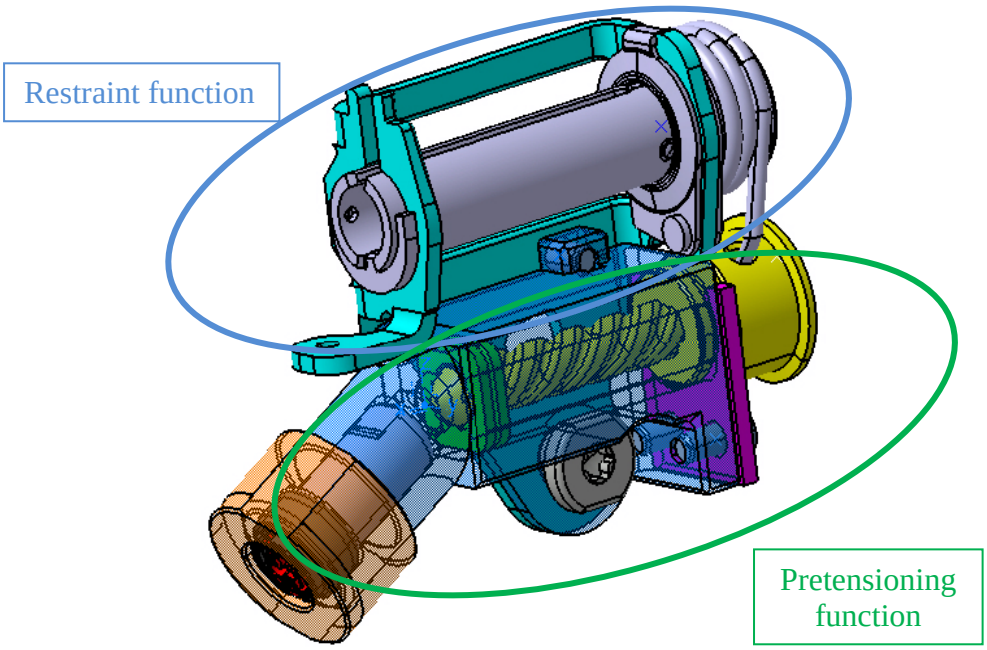

Fig.2. Pretensioning mechanism

The function of the mechanism as shown in *figure 3* is based on the pressure resulted from the gas generator is applied on the surface of the piston, this forces the piston to travel along the combustion chamber in a linear motion and using the thread on the inside acting like a nut and screw mechanism transforms the linear motion into revolutions of the spindle which in turn transmits this energy trough a cable to the webbing spindle.

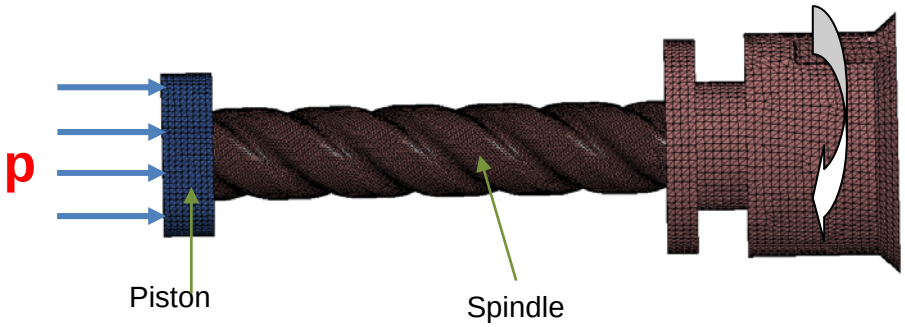

Fig.3. Function of system

3. Test description

The tests were performed on a machine as shown in *figure 4.* The purpose of the test was to measure the torque needed to rotate the spindle for 360º and move the piston.

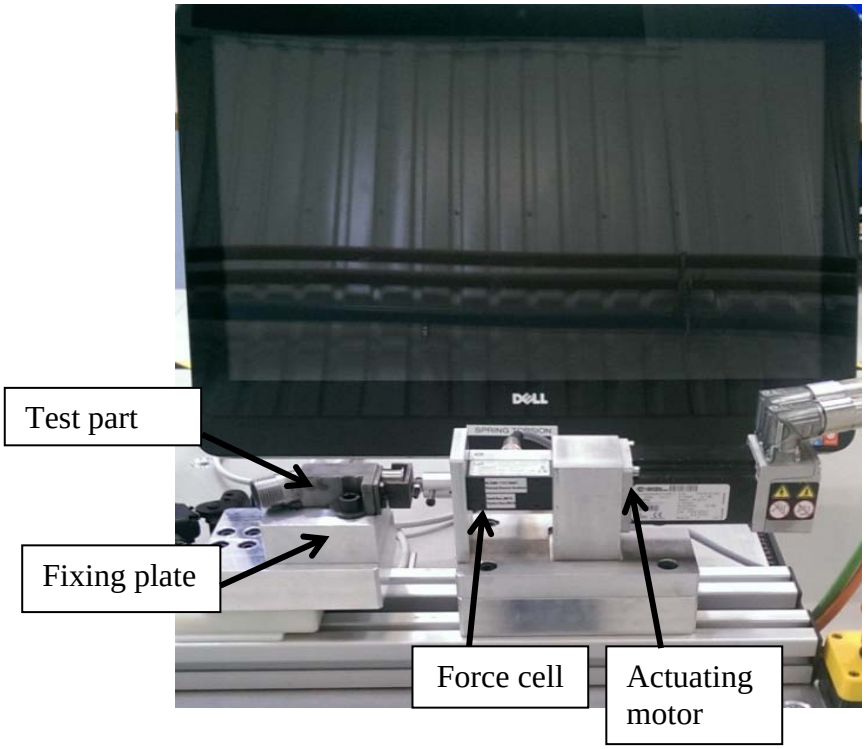

Fig.4. Test machine setup

To assure contact between all the parts I applied a force as shown in *figure 5.* The force applied was 50N and was limited by the recomanded maximum load on the force cell axis.

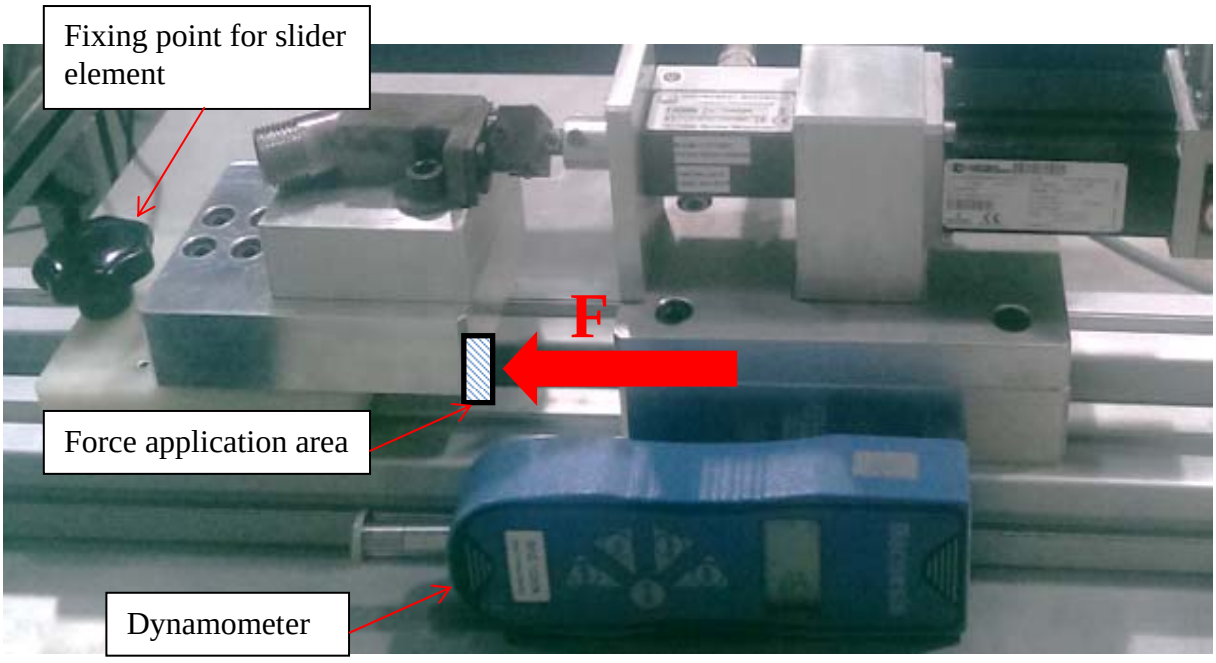

Fig.5. Force applied on the test part

For the test I used 4 different configurations as listed below and I did 10 trials with each variant.

1. Without any lubricant;
2. Lubricated using synthetic oil;
3. Lubricated with grease;
4. A version of the piston with different thread type and using grease as lubricant.

4. Test results and interpretation

Recorded data from the test is in the form of force overtime and I represented it in *graphic 6*, using NI DIAdem to create an overload of the data's obtained from all 4 tests.

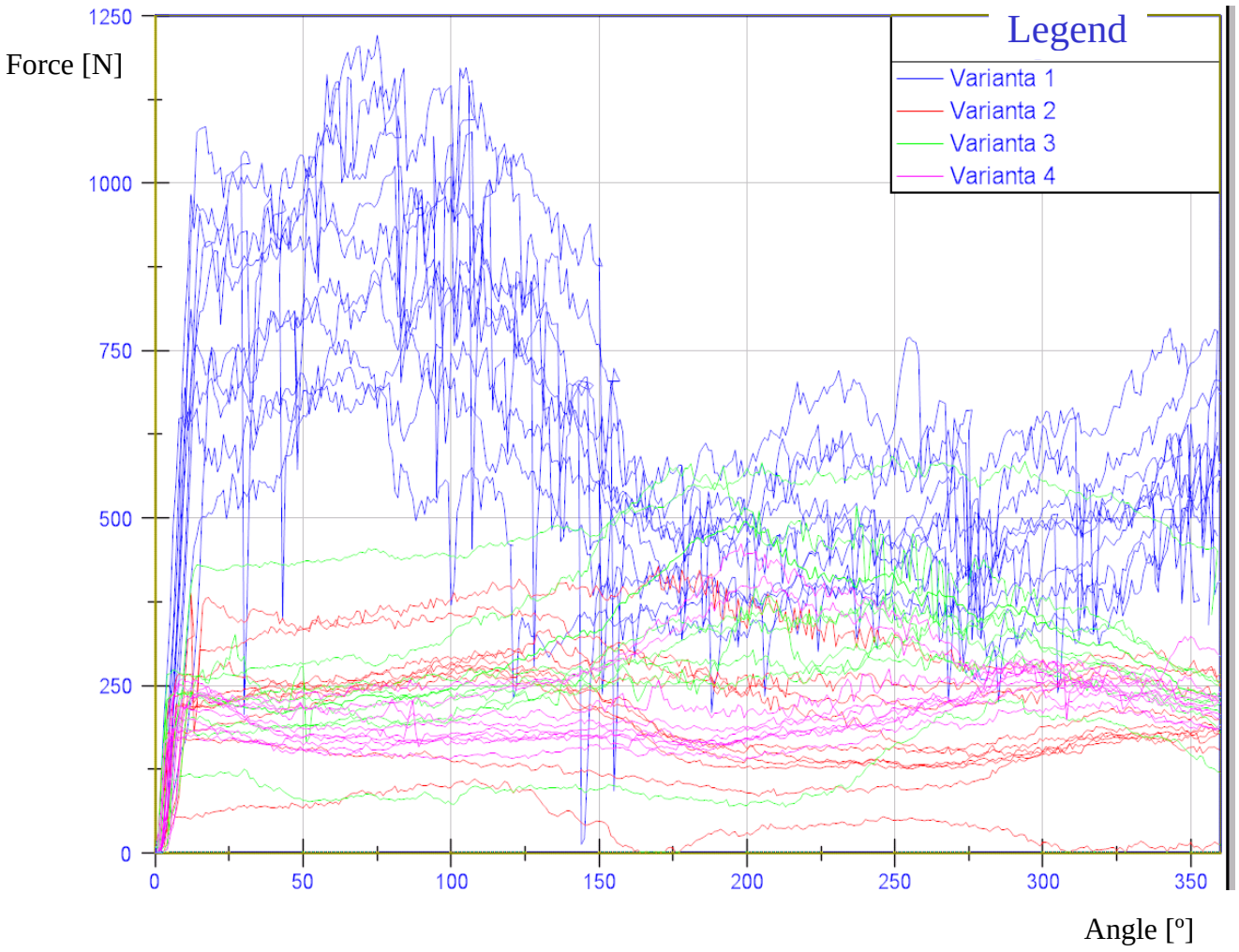

Fig.6. Overloaded graph of obtained data

For the statistical analysis I used the peek force obtained in each trial. The program used for this analysis was MiniTAB and I used it to create a boxplot of the forces to better observe the spread of the values, and a interval plot to be able to determine if there are any significant differences between the value sets, this two graphs are presented in *figures 7*.

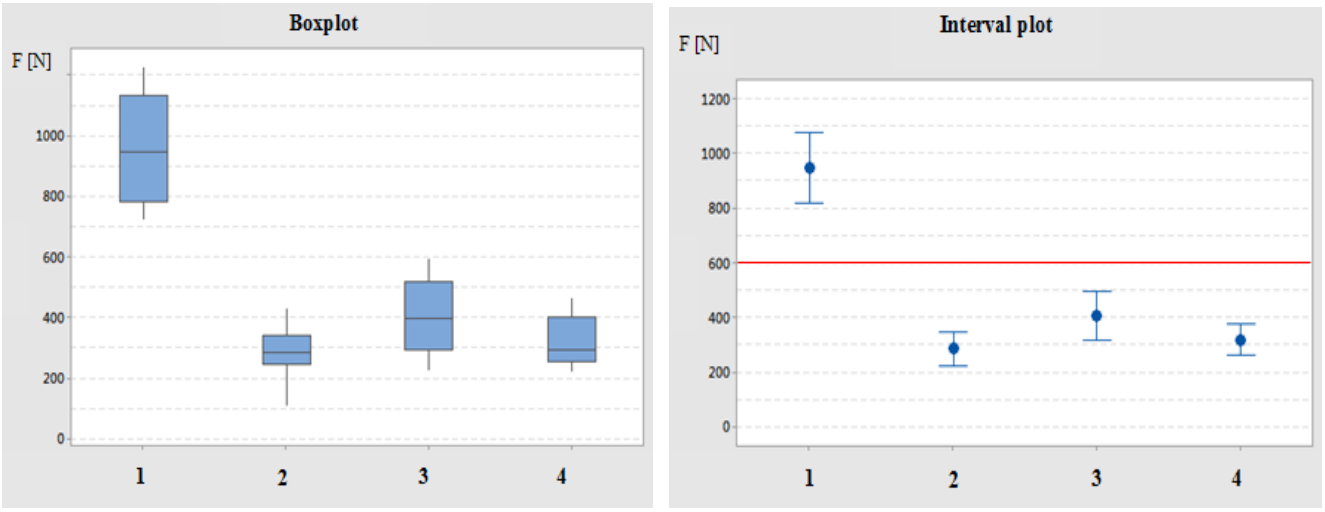

Fig.7. Boxplot and interval plot of maximum force obtained in each trial

The interval plot shows that there is a significant difference between variant 1 and the other 3 variants tested, so from this we can conclude that effect of using a lubricant in the system is a defining factor in order to reduce the forces needed to move the parts in the system.

In the interval plot no significant difference between the other 3 variants so a Two-sample T-test is need in order to see if there is a difference between the 3 sets of values. This test was also performed using MiniTAB. The test results re shown in *figure 8*.

This test is performed for two hypothesis H_0 and H_A. The H_0 (or null hypothesis) considers the data sets to no present any relations, be independent and the values are not different from each other. The H_A (alternative hypothesis) considers the data sets presenting relations, being dependent and the values are different from each other. If the resulting P value is below 0.05 there is a significant difference between the sets with a confidence interval of 95%. [2]

Two-Sample T-Test and CI: Varianta 3, Varianta 4

```
Two-sample T for Varianta 3 vs Varianta 4

                          SE
             N   Mean  StDev  Mean
Varianta 3  10    406    125    40
Varianta 4  10  317.5   80.1    25


Difference = mu (Varianta 3) - mu (Varianta 4)
Estimate for difference:  88.5
95% CI for difference:  (-11.6, 188.6)
T-Test of difference = 0 (vs not =): T-Value = 1.88  P-Value = 0.079  DF = 15
```

Two-Sample T-Test and CI: Varianta 2, Varianta 3

```
Two-sample T for Varianta 2 vs Varianta 3

                          SE
             N   Mean  StDev  Mean
Varianta 2  10  284.6   89.3    28
Varianta 3  10    406    125    40


Difference = mu (Varianta 2) - mu (Varianta 3)
Estimate for difference:  -121.4
95% CI for difference:  (-224.4, -18.4)
T-Test of difference = 0 (vs not =): T-Value = -2.50  P-Value = 0.024  DF = 16
```

Fig.8. Two-sample T-test, variant 3 vs. 4 and variant 2 vs.3

The results of the Two-sample T-test shows that there is a significant difference between the two types of lubricant but there is no significant difference between the two types of piston.

5. Simulation of mechanism

A simulation can be performed on any system, the role of the simulations depends on the needs of the engineer, and they can vary from Finite Element Analysis to assembly and function check.

I this case I need a to prove that using a simulation I can reproduce the real live conditions and that the results are comparable to the tests results obtained and presented in chapter 4.

For the simulation I used the program MSC Adams View, i transferred the 3D CAD models from CATIA to the Adams platform, assembled the parts, set the connections between them and the forces the affected each component, the assembled model is shown in *figure 9.*

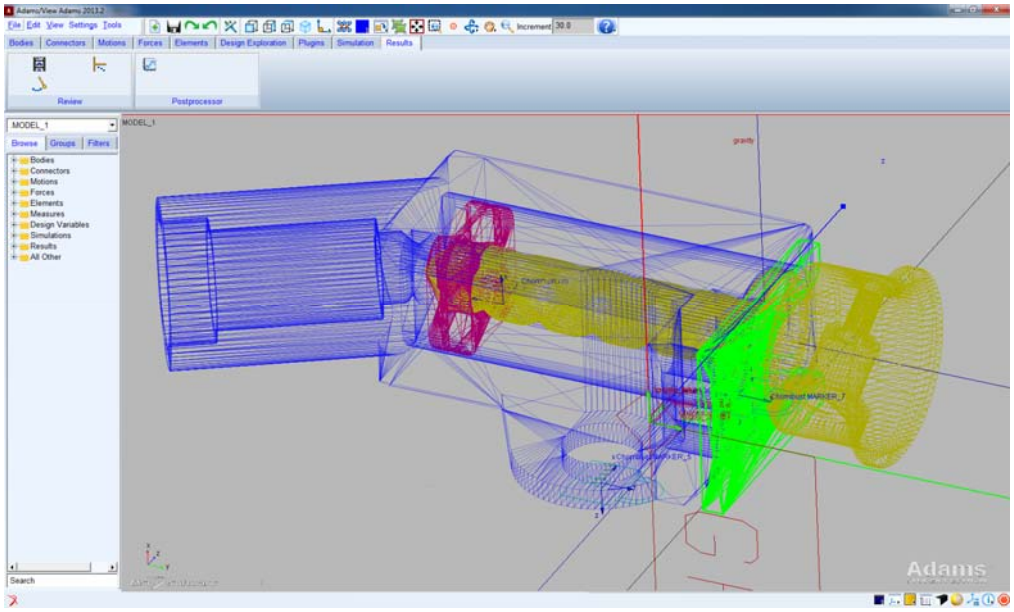

Fig.9. Model prepared for simulation in MSC AdamsView

After performing the simulation the maximum force obtained was 205 N and the graph is shown in *figure 10*. So the results are comparable to the test done in variant 2 and 3 as the friction coefficient used for the simulation was that of lubricated steel parts (0.2).

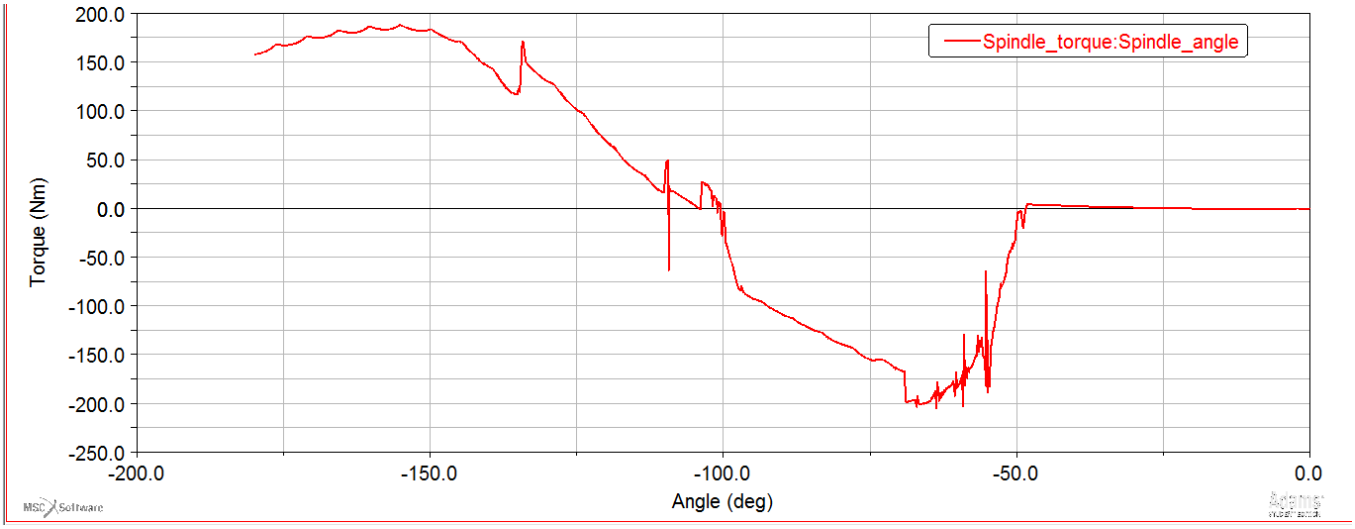

Fig.10. Force graph of the simulation

6. Design of experiment

Design of experiment (DoE), is a 6 sigma method used to be able to distinguish between factors that have an influence on the data obtained and factors that don't have a significant difference.

As presented in chapter 5 the simulation results are relevant and comparable to tests performed on prototypes, so this is used as a baseline for the DoE simulation.

To better understand the influence of 4 factors on the system presented in this paper I performed a DoE using four factors presented in *table 1*.

Table 1. Factors used for DoE

No.	Factor	lower limit	upper limit
1	Friction coefficient	0.2	0.8
2	Piston design	4 corners	8 corners
3	Pitch	0.5	2
4	Time to reach maximum pressure	2 ms	6 ms

The Pareto chart obtained for the factor influence is showed in figure 11. The factors that have a significant influence on the model are the Friction coefficient, the piston design, and a combination between the friction coefficient and piston design.

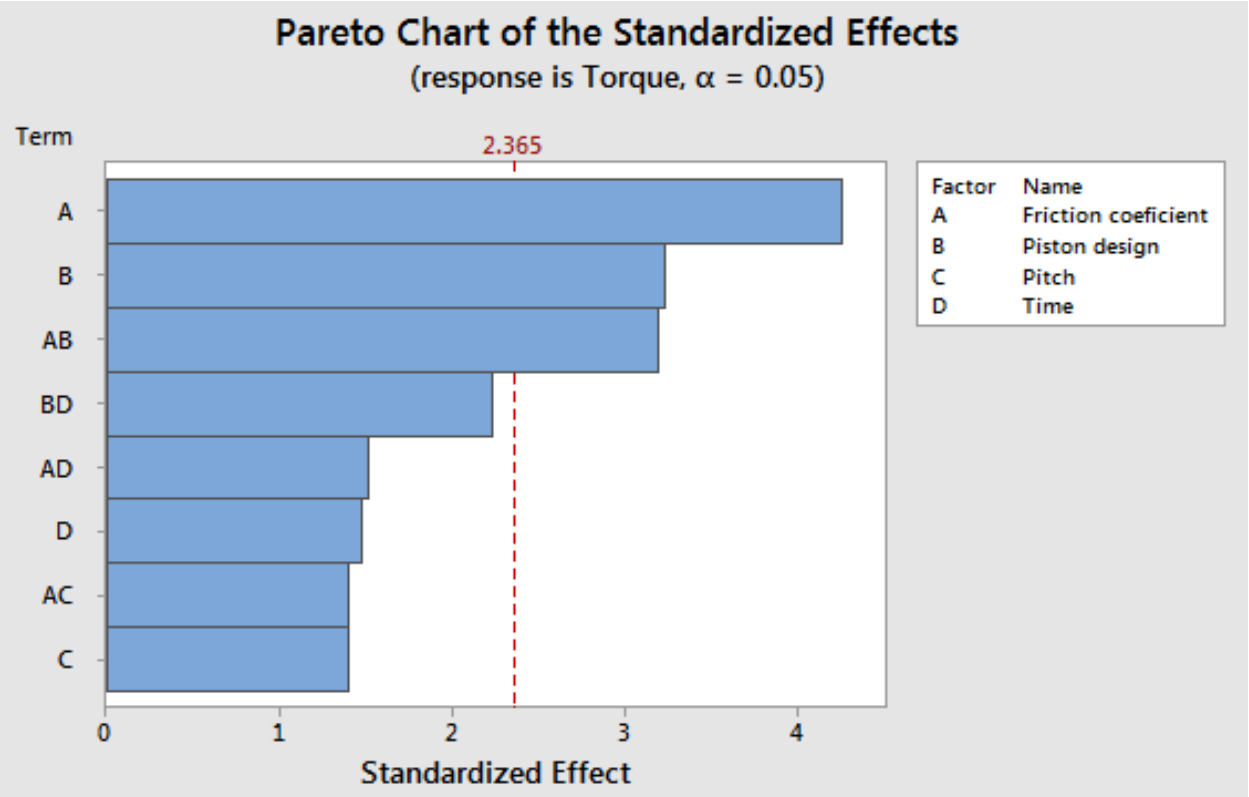

Fig.11. Pareto chart of the standardized effect

7. Conclusions

The tests performed showed the current state of the product and the importance of using a lubricant to reduce the fiction forces between the pats. Also by analysing the result a significant difference was observed between the two different types of lubricant.

The simulations performed showed that the simulation model is comparable to real life experiment bought in setup and results, allowing me to perform a DoE using different factors in the simulation program, as a result saving time and reducing cost for the prototypes and the tests.

The results of the DoE showed me the direction of focus needed to further improve the product with minimal cost and effort.

This paper presents how you can achieve results faster and with a better confidence interval using all the available tools for an engineer, like building prototypes, performing tests, analysing the results using 6 sigma statistical analyses and DoE's and using simulation programs to reduce effort needed for investigating different factors.

REFERENCES

[1] H.Zellmer, C.Kahler, B.Eickhoff, „Optimised pretensioning of the belt system: a rating criterion and the benefit in consumer tests", Autoliv, Elmshorn, Germany, 2001.
[2] R. Meran, A. Jhon, O. Roenpage, C. Staudter, „Six Sigma +Lean Toolset", Springer, Frankfurt, Germany, 2013.
[3] http://amat139unikl.blogspot.ro/2014/05/seat-belt-systems.html

OPTIMIZING THE ENERGY CONSUMPTION OF AN INDUSTRIAL WATER-SUPPLY PUMP SYSTEM BY ENSURING AN OPTIMAL FLOW RATE

Prof. PhD Gencho POPOV[1], PhD Boris KOSTOV[1], PhD Miglena HRISTOVA[1], Asc. Prof. Donka IVANOVA[1], Asc. Prof. Anka KRUSTEVA[1]

[1] University of Ruse "Angel Kanchev", Bulgaria: gspopov@uni-ruse.bg; bkostov@uni-ruse.bg; mcankova@uni-ruse.bg; divanova@uni-ruse.bg; akrasteva@uni-ruse.bg

Abstract: *This work presents theoretical research about the possibilities for achieving at the same time a system's optimal flow and maximum energy efficiency, by using the frequency method of flow rate regulation, with a number of pumps working in parallel. Features, concerning the change of the specific energy consumption, used for the ensuring of different total flow rates in the system, are also indicated. An interesting conclusion is the fact that the minimal energy consumption for the investigated system can be achieved by the realization of different work regimes.*

Keywords*: pump systems, energy efficiency, energy consumption*

1. Introduction

Often, even if the existing requirements for the correct designing of a pump system are being observed, the system doesn't work effectively, which leads to unnecessary energy loses. One of the main reasons for this is the failure to use the full potential of the given system, especially in terms of the utilization of its input power. As a result, finding a way for achieving the optimization of a system's work performance, in terms of energy efficiency, has become a key priority. However, for various reasons, related mainly to the changing consumer needs, it is necessary for the system's flow rate to be increased or decreased, which automatically makes the initial selection of pumps inappropriate. It is well-known that to replace the pump aggregates with new and more effective pumps will be very expensive, so it is necessary to find an alternative solution for this problem.

2. Materials and methods

A scheme of the pump system

The focus of this research is an actual pump system, used for industrial water-supplying, has been selected. Its scheme is given in figure 1. In the designing of this system it was decided that the reservoir, whose volume is 4000 m^3, should be filled with water before the start of the working day, i.e. during the time of its filling there will be no water consumption. Because of the global economic crisis, which began a few years ago, the company which runs this pump system had to reduce their production cycle, reducing daily water consumption by 25%. As a result, a decision was made to exclude one of the existing drilling pumps (P_0), so that the water supply would be provided only by two pumps (P_1) and (P_2). Analogically, in the IInd stage of the pump system only two of the existing three pumps are working – in the designing of this system it was decided that there will be 2 more pumps in reserve (the third pump and the two reserve pumps are not given in figure 1).

Therefore, the initial water supply will be ensured by pumps P_1 and P_2, which are the same type, but located at different heights and distances from each other. Their nominal work parameters are: flow rate - Q=50 l/s; head - H=250 m; induction motor's power - P_M=190 kW; speed of rotation– n=2880 min^{-1}. The main purpose of these two pumps is to ensure the water transportation from Ist to IInd stage. After that the pumps P_3 and P_4: Q=69.5 l/s; H=192; P_M=250 kW and n=1500 min^{-1}, have to ensure the water transportation to the main reservoir. In the designing of the system's IInd stage, it is planned to install a buffer tank, whose volume is 100 m^3. Its main

purpose is to compensate for the different flow rates of the pumps in Ist stage and the pumps in IInd stage.

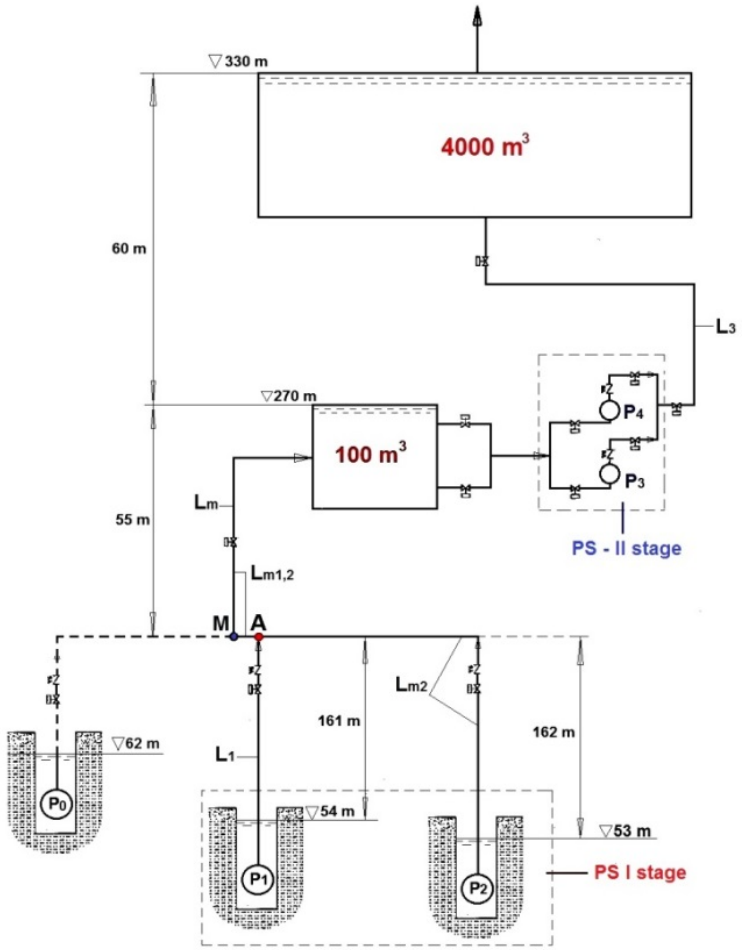

Figure 1 A scheme of the investigated pump system

In table 1 the data for the relative lengths and diameters of each of the pipes forming the pipe system are given.

TAB. 1 Lengths and diameters of the different pipes forming the pipe system

name	length, *m*	diameter, *mm*
L_1	162	273
L_{m2}	812	273
$L_{m1,2}$	2517	-
L_m	1842	325
L_3	1514	325

Structuring of the optimization model

The ensuring of an energy-effective system's work can be possible if the system is divided into two parts: **1** part – from the drilling pumps (P_1, P_2) to the buffer tank; **2** part – from the pumps P_3 and P_4 to the main reservoir). The determination of the flow rate $Q_{opt,1}$ (in **1**) will largely be predestinated and the determination of the flow rate $Q_{opt,2}$, (in **2**) ensured by the pumps P_3 and P_4 – as an additional restrictive condition the volume of the buffer tank and the time for its filling should be selected.

If the characteristics of the pumps and pipe system are known, the determination of the pump system's flow rate shouldn't be a problem. However, this doesn't mean that this will be the most appropriate value, in terms of energy efficiency, where the energy consumption to be minimal. But the optimal value of the flow rate can be achieved, when the two pumps P_1 and P_2 are working together (in parallel), because it is possible to regulate each of them by changing their speed of rotation. In this case, it will be interesting to find out what is the best proportion between the individual flow rates of each of the two pumps, remembering that the total system's flow rate is a sum of these two individual flow rates.

For finding a solution of the hydraulic part of this optimization problem it is necessary to determine (in advance) the work regime, when the pumps P_1 and P_2 work together with their nominal speed of rotations. This can be done by using some well-known hydraulic features (equations) and the method, described in [5]:

- determining the coefficient "k" of the pipe system by estimating the relative coefficient of friction "λ";
- by using equation (1) the (summary) head characteristic (referring to a common point of the pipe system – in this case, it is: p. A – fig. 1) of "n" number of pumps, located in different stations and positioned on different heights, can be found. Therefore, selecting different values of the head H_i, the relevant value of the flow rate Q_i can be estimated by (2):

$$H_i = (a_i - k_i)Q_i^2 + b_i Q_i + c_i - h_i; \tag{1}$$

$$Q_i = \frac{-b_i - \sqrt{b_i^2 - 4(a_i - k_i)(c_i - h_i - H_i)}}{2(a_i - k_i)}, \tag{2}$$

where a_i, b_i and c_i are the coefficients of the head characteristics respectively of a given pump, determined on the basis of the catalogues, provided by the manufacturer; h – the distance between the levels of the water in the exhaustive well and the beginning of the common pipe. For the selected (sample) three different values of the head (H', H'', H'''), taking places in the interval, belonging to the summary head characteristic, the relevant flow rates for each of the parallel working pumps can be estimated by (2) and summed, so to achieve the overall flow rates (Q', Q'', Q'''). This can be used for the determination of the coordinates (Q and H) of three points, belonging to the summary head characteristic. Finding a solution of (3) first and then using (4), (5) and (6) will ensure the determination of the coefficients (a_0, b_0, c_0) of the equation of the summary head characteristic:

$$\begin{vmatrix} H' = a_0(Q_1' + Q_2' + ... + Q_n')^2 + b_0(Q_1' + Q_2' + ... + Q_n') + c_0 \\ H'' = a_0(Q_1'' + Q_2'' + ... + Q'')^2 + b_0(Q_1'' + Q_2'' + ... + Q_n'') + c_0 \\ H''' = a_0(Q_1''' + Q_2''' + ... + Q_n''')^2 + b_0(Q_1''' + Q_2''' + ... + Q_n''') + c_0 \end{vmatrix}; \tag{3}$$

$$b_0 = \frac{(H'' - H''')(Q_{0,1}^2 - Q_{0,2}^2) - (H' - H'')(Q_{0,2}^2 - Q_{0,3}^2)}{(Q_{0,2} - Q_{0,3})(Q_{0,1}^2 - Q_{0,2}^2) - (Q_{0,1} - Q_{0,2})(Q_{0,2}^2 - Q_{0,3}^2)}; \tag{4}$$

$$a_0 = \frac{H' - H'' - b_0(Q_{0,1} - Q_{0,2})}{Q_{0,1}^2 - Q_{0,2}^2}; \tag{5}$$

$$c_0 = H''' - a_0 Q_{0,3}^2 - b_0 Q_{0,3}, \tag{6}$$

where $Q_{01}=Q_1'+Q_2'+\ldots+Q_n'$; $Q_{02}=Q_1''+Q_2''+\ldots+Q_n''$; $Q_{03}=Q_1'''+Q_2'''+\ldots+Q_n'''$ (1, 2...n – parallel working pumps in the system).

Fig. 2 presents graphically the determination of the system's work regime in case the pumps P_1 and P_2 work together on their nominal speeds of rotation:

$$Q_{nom(P1+P2)}=103,6 \text{ l/s},$$

where the work parameters of each of the pumps respectively are:

$$Q_{P1}=51,9 \text{ l/s}, H_{P1}=235,9 \text{ m u } \eta_{P1}=0,76;$$
$$Q_{P2}=51,7 \text{ l/s}, H_{P2}=236,9 \text{ m u } \eta_{P2}=0,76.$$

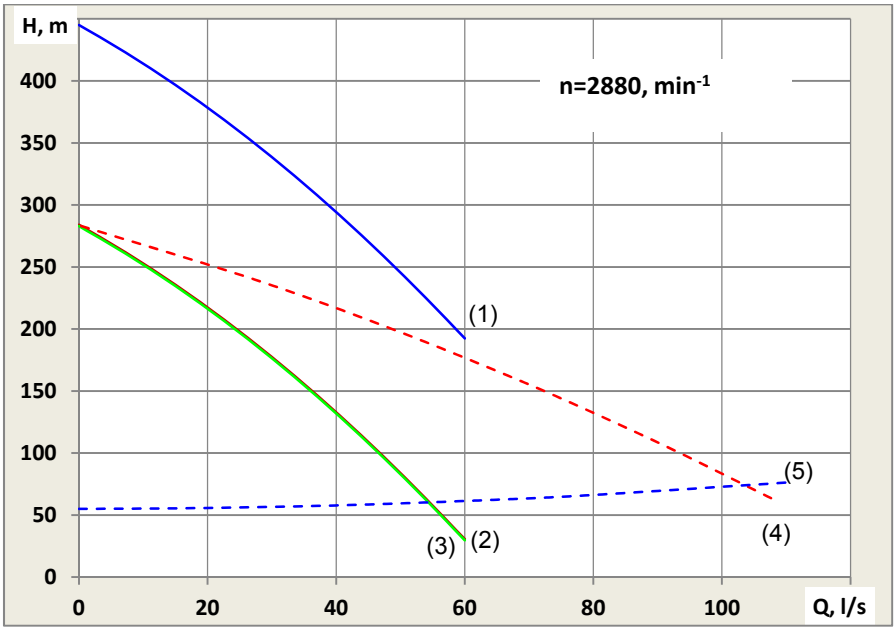

Figure 2. Graphic-analytical determination of the system's work regime, when the pumps P_1 and P_2 work in parallel: (1) pump's head characteristic, provided by the manufacturer; (2), (3) – the head characteristics (referred to p. A) of pumps P_1 and P_2; (4) – the characteristic of the common pipe

For the determination of a system's optimal flow rate, it is necessary to consider the restrictive condition of not allowing too low or high velocity ϑ to be implemented (the existence of too low a velocity leads to the accumulation of sediments in pipes, which interrupts smooth fluid transportation, while the existence of too high a velocity leads to the appearance of corrosion and also causes higher energy loses). That is why as a recommendable standard diapason of allowable velocity values the interval $\vartheta \in 0,75...3$, m/s, is considered, [1]. Considering that the common pipe (in **1**) consists of pipes, having different diameters and the relevant maximum and minimum allowable values, according to the restrictive velocity conditions, the relevant flow rates in these pipes, are determined. As a result, it can be indicated that the total system's flow rate Q belongs to the following interval: $Q \in (0,8\ldots1,15)Q_{nom(P1+P2),}$ m^3/s. The additional verification check indicates that the low boundary condition of the defined interval (for Q) should be changed to 0,9, for the velocities in the pipes, whose lengths are L_1 and L_{m2}, to be valid. It is clear that this final interval for Q represents 100% of the possible flow rates, as for the purpose of this research 4 values, which belongs to it, are selected - $(0,9; 1,05; 1,1; 1,15)Q_{nom(P1+P2)}$. For each of these values, where the total system's flow rate (Q) is being ensured by the two pumps (P_1 and P_2), working in parallel, the investigated ratios between the individual pump's flow rates (Q_{P1}/Q_{P2}) respectively are: 50-50 %; 55-45%; 45-55%; 60-40 %; 40-60 %; 65-35 %; 35-65 %.

For the achieving of the required flow rates, it is necessary for the frequency method of regulation to be used. Therefore, the summary (system's) head characteristic ((3) – fig.2), concerning the two pumps P_1 and P_2 – after they have been referred to the common point A, will intersect the characteristic of the common pipe in different points. Then if the equation $(H'_{(i)}=H_{st}+kQ_{(i)}^2)$, describing the pipe system's characteristic, is known, the estimation of the head

$H'_{(i)}$ (in the common pipe – from p. A to the buffer tank) for the selected values of the flow rate Q_i is possible. The determination of the total head $H_{(P1,2)}$, for each of the parallel working pumps (P_1, P_2), can be achieved by the preliminary determination of the energy losses ($h_{v(i)}$) – for any of the selected values of Q_i, in the pipes (it is also necessary for the impact of the heights - h_1 and h_2, which have to be overcome, to be indicated):

$$H_{(P1,2)} = H'_{(P1,2)} + h_{v(P1,P2)} + h_{(1,2)},\ m. \tag{7}$$

To determine the coefficient of efficiency for each of the pumps (P_1, P_2), remembering the fact that after the change in the speed of rotation there will be a new work regime, it is necessary for the new speed of rotation to be determinate in advance. For this aim the graphic-analytical method, described in [2], where the parabola of similarity, which is a key factor (it is assumed that a given pump works at the same value of its coefficient of efficiency for all the ensured similar work regimes), can be used. The results, found after the completion of the hydraulic calculations, representing the parameters of the new work regimes, are given in table 2.

TAB. 2 Work parameters of the provided new work regimes

$Q=0,9.Q_{(P1+P2)}$	**P_1+P_2**		**P_1+P_2**		**P_1+P_2**		**P_1+P_2**		**P_1+P_2**	
$Q_1:Q_2$, %	**50-50**		**55-45**		**45-55**		**60-40**		**40-60**	
Q, m^3/s	0,047	0,047	0,051	0,042	0,042	0,051	0,056	0,037	0,037	0,056
H, m	220,35	223,01	221,26	221,87	219,52	224,27	222,26	220,85	218,78	225,65
η	0,78	0,78	0,75	0,78	0,78	0,75	0,70	0,77	0,77	0,71
n, min^{-1}	2714	2720	2810	2631	2621	2796	2911	2542	2533	2924
e_V, kWh/m^3	0,774	0,783	0,804	0,773	0,765	0,819	0,866	0,779	0,771	0,872
$Q=1,05.Q_{(P1+P2)}$	**P_1+P_2**		**P_1+P_2**		**P_1+P_2**		**P_1+P_2**		**P_1+P_2**	
$Q_1:Q_2$, %	**50-50**		**55-45**		**45-55**		**60-40**		**40-60**	
Q, m^3/s	0,054	0,054	0,060	0,049	0,049	0,060	0,065	0,044	0,044	0,065
H, m	221,92	225,18	223,16	223,63	220,79	226,90	224,52	222,23	219,79	228,78
η	0,72	0,72	0,64	0,77	0,77	0,65	0,53	0,78	0,78	0,54
n, min^{-1}	2877	2890	2997	2773	2762	3011	3121	2662	2652	3137
e_V, kWh/m^3	0,841	0,848	0,951	0,794	0,786	0,954	1,164	0,774	0,766	1,153
$Q=1,1.Q_{(P1+P2)}$	**P_1+P_2**		**P_1+P_2**		**P_1+P_2**		**P_1+P_2**		**P_1+P_2**	
$Q_1:Q_2$, %	**50-50**		**55-45**		**45-55**		**60-40**		**40-60**	
Q, m^3/s	0,057	0,057	0,063	0,051	0,051	0,063	0,068	0,046	0,046	0,068
H, m	222,50	225,98	223,86	223,43	221,26	227,86	225,36	222,75	220,16	229,93
η	0,69	0,69	0,58	0,75	0,75	0,60	0,45	0,78	0,78	0,47
n, min^{-1}	2933	2947	3061	2819	2810	3076	3194	2703	2693	3211
e_V, kWh/m^3	0,885	0,890	1,045	0,838	0,830	1,166	1,377	0,779	0,770	1,347
$Q=1,15.Q_{(P1+P2)}$	**P_1+P_2**		**P_1+P_2**		**P_1+P_2**		**P_1+P_2**		**P_1+P_2**	
$Q_1:Q_2$, [%]	**50-50**		**55-45**		**45-55**		**60-40**		**40-60**	
Q, m^3/s	0,060	0,060	0,066	0,054	0,054	0,066	0,071	0,048	0,048	0,071
H, m	223,10	226,81	224,59	224,95	221,75	228,87	226,23	223,28	220,54	231,13
η	0,64	0,65	0,52	0,73	0,73	0,53	0,36	0,77	0,77	0,38
n, min^{-1}	2991	3005	3127	2873	2860	3143	3268	2746	2735	3286
e_V, kWh/m^3	0,944	0,947	1,178	0,838	0,830	1,166	1,731	0,787	0,779	1,657

The results found in this research make it clear that because of the imposed restrictive condition, concerning the velocity of fluid's transportation through the pipes, the work regimes at Q_{P1}/Q_{P2}= (65:35 and 35:65 %), are not available.

As a key factor, determining the effectiveness of the system's work performance the specific energy consumption e_V, is selected. According to [4], it can be estimated by (8):

$$e_V = (g/3600).(H/\eta),\ kWh/m^3 \tag{8}$$

where H is the pump's head, $\eta=\eta_E\eta_T\eta_P$ - the total coefficient of efficiency of the pump aggregate (it is assumed that the motor's coefficient of efficiency has a constant value [3], and the transmission's coefficient of efficiency is equal to 1).

After the completion of the estimations, used to determine the specific energy consumption $e_{V(i)}$ for each of the required work regimes, it has been presented as a dimensionless parameter. For this aim $e_{V(i)}$ has been referred to the specific energy consumption e_{Vnom}, which is realized when the pumps (P_1 and P_2) work on their nominal speed of rotation (n=2880 min^{-1}).

3. Results and discussion

Figure 3 graphically presents the change of the relative specific energy consumption $e_{V,отн}$ for different ratios between the flow rates (Q_{P1} and Q_{P2}) of the pumps P_1 and P_2, when the values of the system's total flow rate are preliminary asked.

Figure 4 graphically presents the relative specific energy consumptions $e_{V,отн(i)}$, provided at same asked values of the ratio between the flow rates of the pumps P_1 and P_2, for the required values of the system's total flow rate.

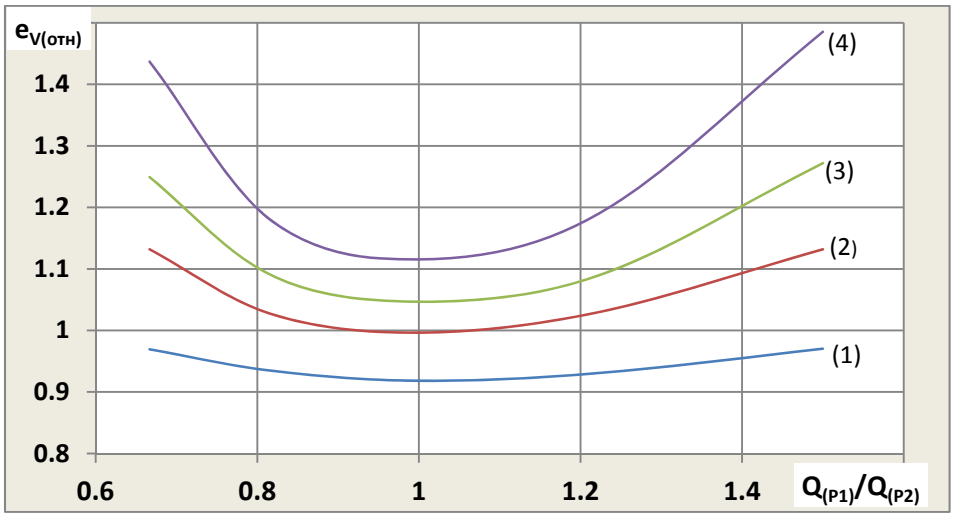

Figure 3. Change in the relative specific energy consumption e_{VOTH}, for different ratios between the flow rates Q_{P1} and Q_{P2}, ensured by the pumps P_1 and P_2: (1) - $Q=0,9Q_{nom}$; (2) – $Q=1,05Q_{nom}$; (3) – $Q=1,1Q_{nom}$; (4) – $Q=1,15Q_{nom}$

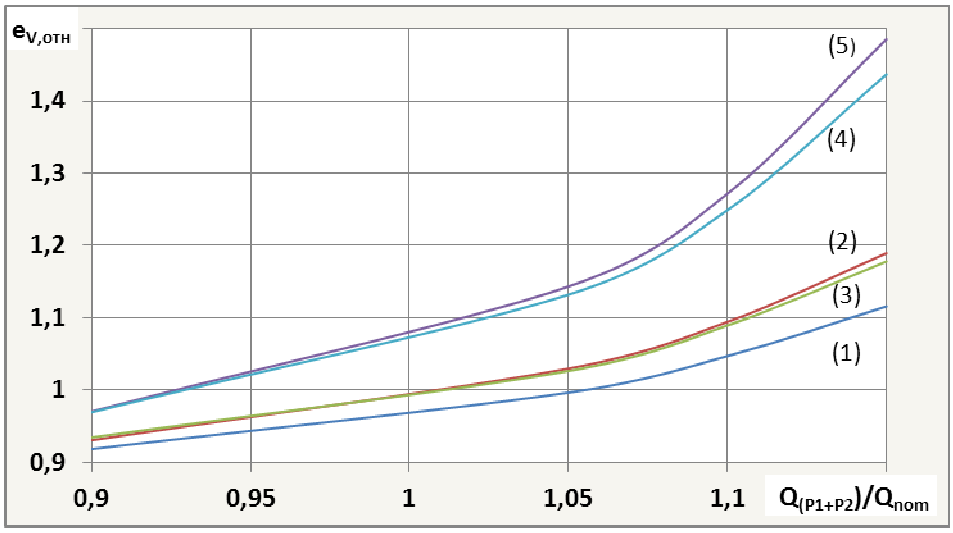

Figure 4. Relative specific energy consumption for the investigated ratios of Q_{P1}/ Q_{P2}, when the system's total flow rate changes: (1) – 50-50%; (2) – 55-45%; (3) – 45-55%; (4) – 60-40%; (5) - 40-60%

Figure 4 graphically presents the relative specific energy consumptions $e_{V,отн(i)}$, provided at same asked values of the ratio between the flow rates of the pumps P_1 and P_2, for the required values of the system's total flow rate.

Analyzing the results found in fig. 3, it can be clearly seen that with the increasing of the system's total flow rate Q the energy, used for the transportation of 1 m^3 of water, also start to increase. This happens faster, when: $Q_{P1}/Q_{P2}<0,8$ and $Q_{P1}/Q_{P2}>1,2$. The increased energy consumption, when the system's total flow rate has been increased, can be explained with the fact that the energy losses in the pipe system are also increased. Because of the significant length of the pipes these losses can be defined as one of the key factors, having an impact on the head of the pumps, respectively on their specific energy consumptions. While the above statement is expected, it is more interesting to indicate that for all the investigated work regimes, independently of the change of Q, (for a given pump system (and pumps)), the specific energy consumption will be minimal at $Q_{P1}/Q_{P2} \approx$ 50-50%. Whether this conclusion is valid for a wide range of pumps, or it is true only for this particular case, could be found when additional research, where different combinations of pumps are provided, is accomplished.

For the given pump system the optimal value of the relative specific energy consumption will be $\mathbf{e_{V,отн} \approx 0,92}$, which represents the minimum of the function of equation (9), describing curve (1) – fig. 3:

$$e_{V,отн} = -0,2181(Q_{P1}+Q_{P2})^3 + 0,9968(Q_{P1}+Q_{P2})^2 - \\ -1,353(Q_{P1}+Q_{P2}) + 1,4929. \quad (9)$$

The results, graphically presented in fig. 4, confirm the tendency that $e_{V,отн}$ increases with the increasing of the system's total flow rate ($Q_{(P1+P2)}$). More interesting in this case is for the change of $e_{V,отн}$, when a given flow rate is ensured at different values of the ratio Q_{P1}/Q_{P2}, to be indicated. Over again, $Q_{P1}=Q_{P2}$ can be determinate as the most appropriate distribution between the flow rates of P_1 and P_2. Also, it can be seen that for both the "mirror" ratios (55-45↔45-55; 60-40↔40-60), when the system's total flow rate has a constant value, the values of $e_{V,отн}$ are very similar, almost covering each other at $Q_{(P1+P2)}=(0,9...1).Q_{nom.}$ However, at $Q_{(P1+P2)}>Q_{nom}$ the difference between the values of $e_{V,отн}$ starts to increase.

A better imagination for the change of $e_{V,отн}$, when the frequency method of flow rate regulation is used, can be ensured if the graphs, presented in figures 3 and 4, are being combined in a common three-dimensional graph (fig. 5). In this graph the $e_{V,отн}$ is presented as a function of two parameters - Q_{P1}/Q_{P2} and $Q_{(P1+P2)}/Q_{nom}$.

For this aim with the help of Matlab a mathematical model is established. Using this model make it possible for a given number (17) of curves, describing the presented spatial plane, to be found. The model representing the relation between $e_{V,отн}$ and Q_{P1}/Q_{P2}; $Q_{(P1+P2)}/Q_{nom}$, is given by (10):

$$e_{v,отн} = 1/(b_1 + b_2(Q_{P1}/Q_{P2} + b_3(Q_{P1}/Q_{P2})^2) + b_4 + \\ b_5 Q_{P1}/Q_{P2} + b_6(Q_{P1}/Q_{P2})^2 + b_7(Q_{P1}/Q_{P2})(Q_{(P1+P2)}/Q_{nom}) + \\ + b_8(Q_{(P1+P2)}/Q_{nom}) + b_9, \quad (10)$$

where the values of the coefficient b are given in Table 3.

TAB. 3 Values of the coefficient, taking place in model: $e_{V,отн}=f(Q_{P1}/Q_{P2}, Q_{(P1+P2)}/Q_{nom})$

b_1	b_2	b_3	b_4	b_5	b_6	b_7	b_8	b_9
0.6700	0.9002	3.0907	0.2134	-1.6840	0.7584	0.3838	0.8563	0.2134

The coefficient of correlation between the estimated and predicted (according to the established model) values of the relative specific energy consumption is R=0.9297. Using the Student's t-criteria the significance of the coefficient of correlation is found.

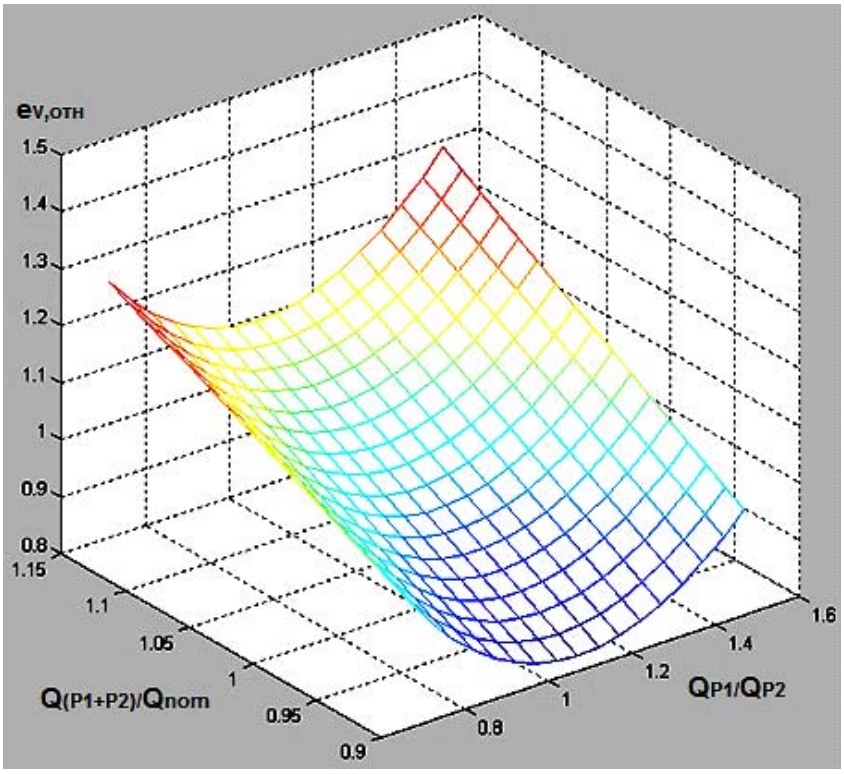

Figure 5. Change of the relative specific energy consumption $e_{V,отн}$, presented as a function between Q_{P1}/Q_{P2} and $Q_{(P1+P2)}/Q_{nom}$

In fig. 5 it can be clearly seen the existence of different work regimes, belonging to the defined working area, where the energy consumption has the same value $e_{V,отн}$=const. The curves, found by (9), consisting of that kind of work regimes, are given in fig. 6.

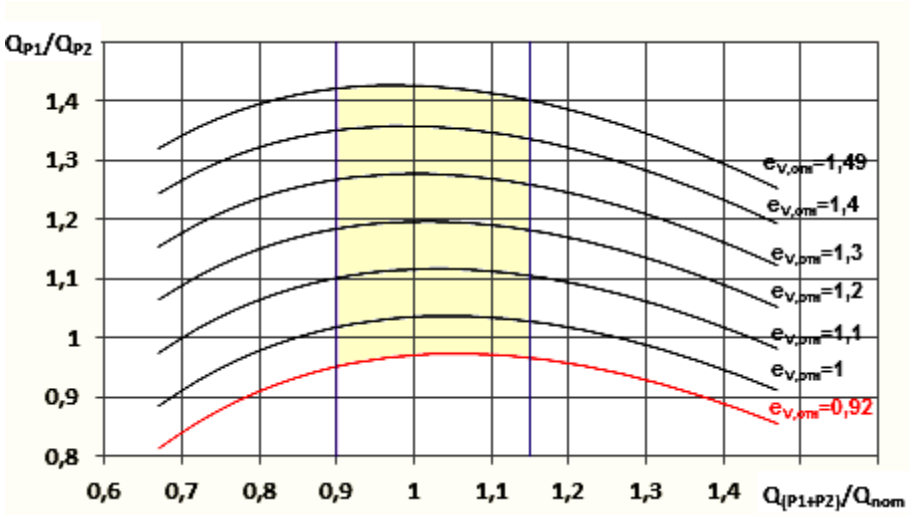

Figure 6. Curves of constant relative specific energy consumption

Analyzing the results found in fig. 6, we can see the interesting fact that the minimal (relative) specific energy consumption (the red line) – for a given system, can be ensured by providing different system's total flow rates, in case that some strictly regulated ratios between the flow rates of P_1 and P_2 are met.

The determination of the optimal flow rate for the second part of the pump system can be done in a similar manner, however it is necessary for the capacity of the buffer tank to be indicated.

4. Conclusions

According to this research, the following are the most important conclusions:

- the established method for the determination of the optimal system's flow rate, in terms of energy efficiency, can be applied for any given pump system;
- after some trends about the change in the specific energy consumption, provided for the ensuring of different system's flow rates, which also are distributed differently between the two supplying pumps, are indicated, the next step is to investigate whether these trends are valid only in this particular case or can be used in general;
- it is proved that the system's minimal (relative) specific energy consumption can be provided by the ensuring of different work regimes.

REFERENCES

[1] Designing norms of water-supply systems, ABC Technics Ltd., 2003
[2] Popov G., Basic data and investigation of the energy efficiency of pump systems, University of Ruse, 2008
[3] Popov, G., Klimentov Kl., Kostov B., "Methods to estimate the energy consumption in regulating the flow rate of pump systems". DEMI'2011, Banja Luka (Bosnia), 2011, pp. 495-500
[4] Burt C., Piao X., Gaudi F., Busch B., Electric Motor Efficiency under Variable Frequencies and Loads, California, USA, 2006
[5] Popov, G., A. Krasteva, B. Kostov, D. Ivanova, Kl. Klimentov, Optimization of the energy consumption of a pump system used for industrial water supply. Annals of faculty engineering Hunedoara – international journal of engineering, Tome XII ISSN: 1584-2665, Romania, 2014

TWO OPERATING MODES ELECTRO-HYDRAULIC SERVO VALVE

PhD. eng. Teodor Costinel POPESCU[1], Dipl. eng. Alina Iolanda POPESCU[2]

[1,2] National Institute for Optoelectronics, INOE 2000-IHP Bucharest,

[1] popescu.ihp@fluidas.ro ; [2] alina.ihp@fluidas.ro

Abstract: *This material refers to a new type of hydraulic equipment for proportional distribution of the working fluid, electro-hydraulic servo valve type, which can work also in high adjustable frequency, through remote electronic control. The equipment, which can be used in precision hydraulic systems, particularly those with automatic operating mode, is patent pending. It offers several advantages over conventional solutions and can operate in two operating modes: as an electro-hydraulic device for proportional distribution of the working fluid, and as an electro-hydraulic distribution device of high adjustable frequency.*

Keywords*: electro-hydraulic servo valve, proportional distribution, high adjustable frequency*

1. Introduction

There are known electro-hydraulic servo valves, consisting of a body in which there slides a distribution slide valve, driven by the pressure created on its ends by a "nozzles - clack valve" unit, receiving the oscillation motion from a " torque motor ", consisting of two electric coils and a metal fitting, but these devices have the following disadvantages: the need for special filtration of the working fluid, permanent loss of pressure through nozzle chokes, generating excessive oil heating, even in the non-actuated position, and a complex electronic actuation device called servo controller, which further increases the already high cost price of servo valves.
There are also known electro-hydraulic proportional directional control valves, consisting of a body in which there slides a distribution slide valve, to which there are attached two proportional control solenoids, but they have the disadvantage that they cannot operate at high frequencies of oscillation, having high attenuation.
The technical problem solved by this new type of servo valve [1] consists in eliminating the nozzles - clack valve unit, which used to lead to a fine filtration of the working fluid and large pressure losses, this unit being replaced by a drive system made up of a proportional reduction piston, a reversal slide valve and a cam rotary oscillator, leading to very inexpensive electronic control device and servo valve construction, that can operate also at very high frequencies without recording a measurable attenuation.

2. Force feedback electro-hydraulic servo valve

Figure 1 shows the construction and operation of the most representative type of hydraulic servo valve: force feedback two-stage electro-hydraulic servo valve. The device comprises three systems, namely:
The control system, electromechanical converter type, positioned on the upper level, which is made up of a torque motor with two electrical coils, a mobile fitting and a fixed fitting. If at this system an electrical input is applied, namely supply current for a coil, this results in a mechanical output, namely mobile fitting movement proportional to the intensity of the supply current of the coil. The mobile fitting, which has a widened area in the form of a blade, moves to the left or right, depending on which coil is supplied with current.
The nozzle-blade preamplifier, mechanical-hydraulic converter type, positioned on the middle level, which is a double hydraulic potentiometer, consisting of a body, where two calibrated nozzles are placed, a blade integral with the mobile fitting of the torque motor and two adjustable hydraulic resistances (throttles). If at this system a mechanical input is applied, namely blade movement towards one or the other of the two nozzles (depending on the amount of the current and which

electric coil of the torque motor is supplied), this results in a hydraulic output type differential pressure between the supply circuits of these nozzles. This differential pressure is caused by the blade getting close to one nozzle (pressure increases) simultaneously with distancing from the other nozzle (pressure decreases), when it is driven to move from its null position.

The distribution system, hydro mechanical converter type, consisting of a body, in which there can move linearly a four arms sliding cylindrical valve, and by this movement there is achieved the communication area controlled, between the pressure circuits (P), provided with two filters, and the return circuit (T) with consumer circuits (A and B). The movement of the distribution sliding valve in magnitude and direction is proportional to the pressure difference applied on its ends.

The force feedback of servo valve is provided by a flat spring, integral with the mobile fitting of the torque motor and the blade of the nozzle-blade preamplifier. The spring has at its end a metal ball by which it is fixed in a housing made in the central area of the distribution spool valve. The servo valve ensures proportionality between the supply current of the torque motor windings and the flow on consumers A or B.

The disadvantages of this type of servo valve that the new type intends to remove are:

- **excessive filtration of oil**, due to the possibility of partial or total plugging of the calibrated nozzles;
- **Permanent loss of pressure** through the nozzle-blade preamplifier, as a result of continuous oil flow through the two calibrated nozzles, which leads to additional heating of the hydraulic oil;
- **the high cost of the electronic control device** type servo controller.

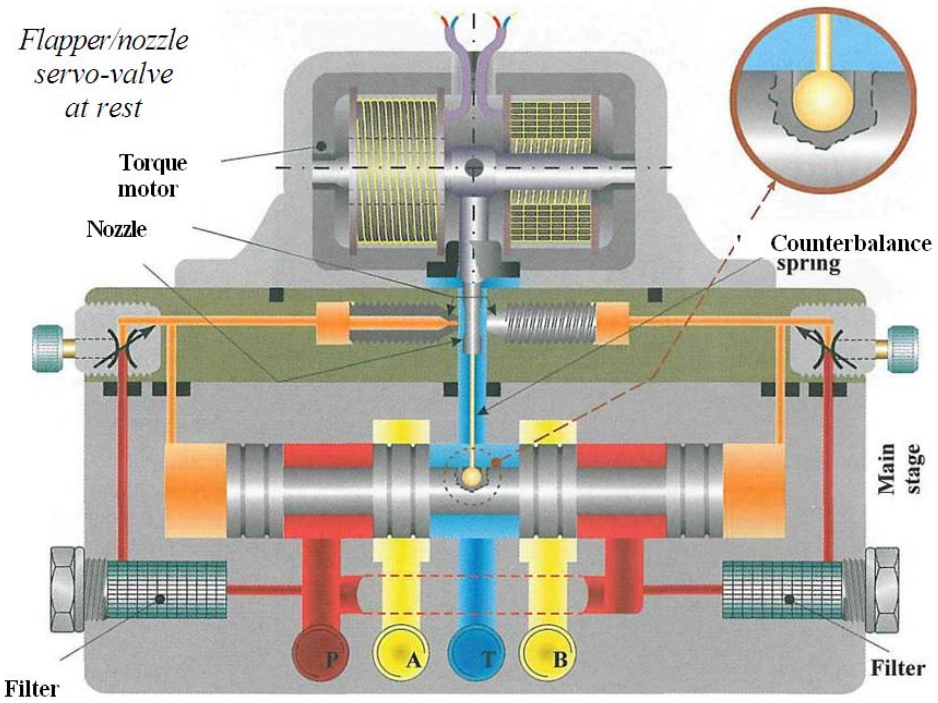

Fig.1 Force feedback electro-hydraulic servo valve

3. Internal position feedback 4/3 proportional directional control valve

4/3 proportional directional control valves can be directly controlled or pilot-operated, with one or two proportional solenoids, with or without electronic control unit. Figure 2 shows a modern 4/3 proportional directional control valve, directly controlled, with two proportional solenoids, internal position feedback provided by means of an electronic control unit and a linear displacement LVDT type transducer.

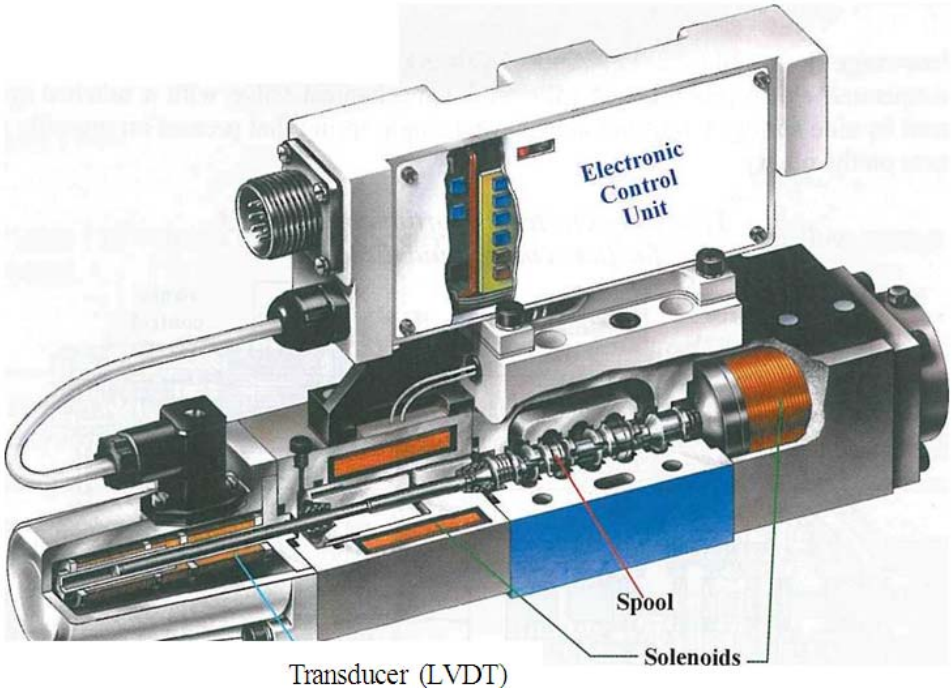

Fig.2 Internal position feedback 4/3 proportional directional control valve

The disadvantages of this type of electro-hydraulic proportional **directional control valves**, which the proposed solution removes, relate to **the relatively high price** and the fact that **they can not operate at high oscillation frequencies**, having high attenuation.

4. Structure of the two operating modes electro-hydraulic servo valve

The two operating modes electro-hydraulic servo valve, Figure 3, Figure 4, Figure 5, is composed of a body closed by two caps, between which there can slide a spool and a distribution bushing. The spool and the bushing are kept in the middle position by two springs per each. The spool can be brought into an initial position, the null, by a screw present in one of the two caps, or by actuating with a control pressure, created by a proportional reduction piston and distributed by a reversing slide valve, both present in the second cap. The bushing can also be actuated by a cam rotary oscillator, mounted on top of the servo valve body.
This hydraulic servo valve has the following advantages:
- it does not have pressure losses, at rest in the middle position, which leads to the elimination of permanent cooling of the working fluid;
- filtration of working fluid (hydraulic oil in this case) can be normal, with a fineness of 25 microns;
- the use of a single proportional solenoid, associated with a reduction slide valve, of a reversing solenoid, and also of a cam rotary oscillator, driven by a variable speed small motor, leads to a cheap constructive solution both for the servo valve and the electronic control device required;
- to the upper speed limit of the cam oscillator, attenuation of fluid distribution in frequency is almost zero, there being possible to achieve very high working frequency (about 200 Hz).
The body **1** of the servo valve, parallelepiped shape, is closed on the left side with a cap **2** and on the right side with another cap **3**, in which there is a bushing **4**, sliding between two springs **5.1** and **5.2**. In the bushing there is a distribution spool **6**, which is positioned between two more springs **7.1** and **7.2** which rest on a washer **8** and a plate **9**, being in constant contact with an adjustment screw **10**. The screw **10,** located in the cap **2**, is held in place by a nut **11** and protected by a small cap **12**.
The body **1** can be adjusted by means of screws on a block of hydraulic circuits, not shown, as it has five ports for connections, noted and arranged according to the international rules: **P**- pressure circuit, **A** and **B** – consumer circuits, **T** (two ports) - return circuits. In the body **1** these ports communicate with ducts made in the bushing **4**, like this: **P** with **d**, **A** with **e**, **B** with **f** and **T** with **g**.

Also in the body **1** there is made a hole, which communicates with the port **P** and makes the connection with a duct **a**, located in the cap **3**, interconnecting in its turn to a reduction piston **14** seating, which is in contact with the rod of a proportional solenoid **13**.

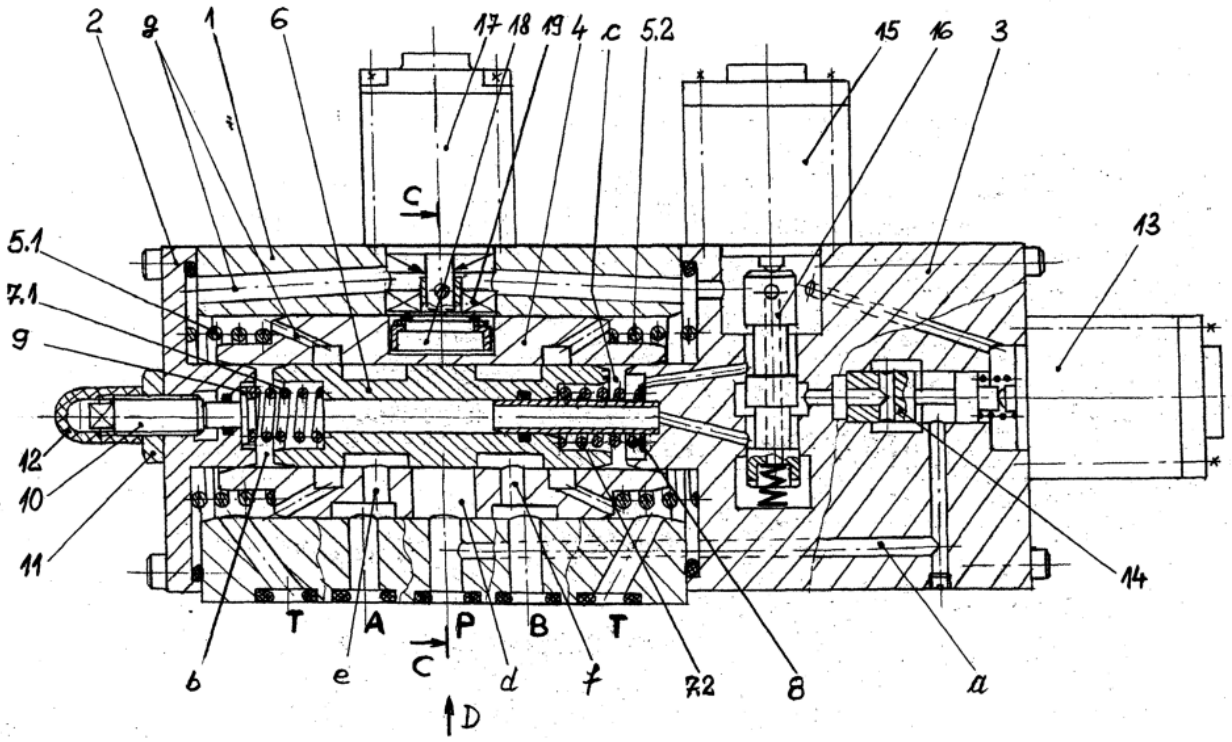

Fig.3 Longitudinal section through the two operating modes electro-hydraulic servo valve

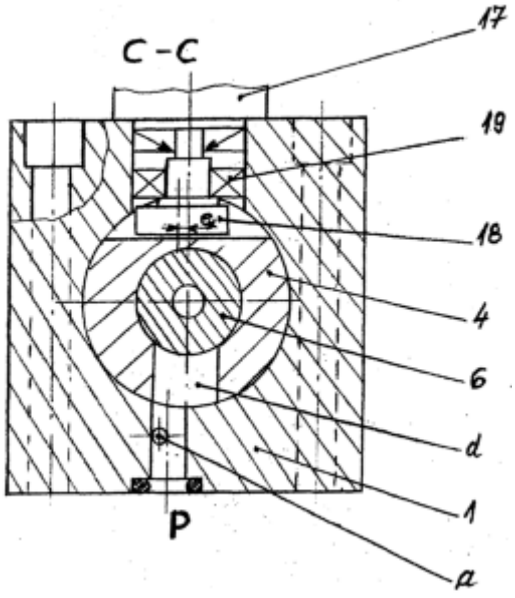

Fig.4 Cross section in the oscillator

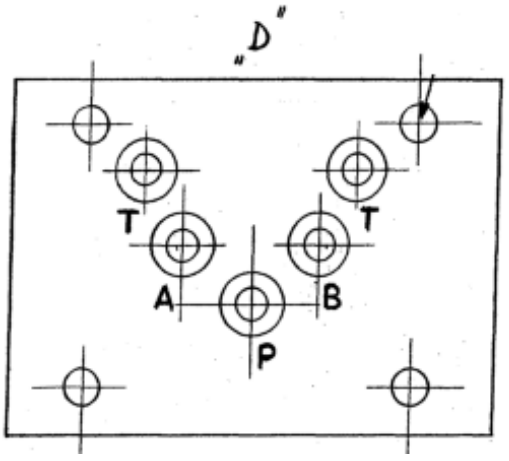

Fig.5 Clamping of the servo valve international mirror

In the cap **3** there is also a reversal spool **16**, held by a spring in contact with the rod of another solenoid **15**, for switching, which can link the output of the reduction piston **14** to a control chamber **b**, or another control chamber **c**, located at the ends of the spool **6**.
The bushing **4** has a milled slot, in the middle, on outer surface and opposite to the duct **d**, where there is a rotary cam **18**, fixed to the shaft of a small motor **17**, reinforced with a bearing **19**, mounted in a seating at the upper side of the body **1**.

5. Functioning of the two operating modes electro-hydraulic servo valve

Functioning of the servo valve is as follows:
At rest, or null position, the servo valve in terms of construction and functioning can have two types of hydraulic coverage: positive coverage, when all holes (P, A, B and T) are closed, or negative coverage, when all holes are in throttled communication, equal crossing sections. To achieve this state, remove the protection small cap **12**, loosen the nut **11** and operate the screw **10**, so that the spool **6** is in the middle position, then tighten the nut **11** for locking.
At functioning as proportional distribution hydraulic equipment, the servo valve must be capable of distributing from port **P** to port **A** or to port **B** a fluid flow proportional to an electric control current.
Proportional distribution is done as follows: the solenoid **13** is power supplied; it drives the piston **14**, which generates at its output a pressure + the inlet pressure of the duct **a**, but proportional to the control current. This reduced pressure is applied to the end of the spool **6**, in the control chamber **b** and produces a force which moves the spool to the right, opposite to the spring **7.2**, making communications **P** to **A** and **B** to **T**, opening section and flow being proportional to the control current.
When supplying the solenoid **15**, it drives the spool **16,** which moves downwards, against the supporting spring, and allows the installation of low pressure in the control chamber **c,** which produces a force that causes the spool **6** to move to the left, against the spring **7.1**, this time making communications **P** to **B** and **A** to **T**, opening section and flow also being proportional to the control current (applied to the same solenoid **13**).
At functioning in frequency, which in the existing servo valves is synonymous with response to a sinusoidal electrical signal, for example, the servo valve must supply from the port **P** the ports **A** and **B**, successively, with prescribed and adjustable frequency. This happens as follows: this time there is supplied the small motor **17**, which rotates the cam **18** and causes the bushing 4 to move left and right, and the spool **6** being fixed, by movement of the bushing there is achieved distribution **P** to **A** and **B** to **T**, respectively **P** to **B** and **A** to **T**, successively, with a frequency equal to the speed of the small motor **17**, which can be adjusted via the control electric current. By canceling the control current applied to the small motor **17**, it stops, and the bushing **4** returns to its initial position, being brought by the springs **5.1** and **5.2**, which does not allow the cam **18** to remain in any position.

6. Conclusions

- With this material the authors test the market of those interested in producing a new type of electro-hydraulic servo valve, cheaper and higher energy efficiency, cumulating two functions, proportional distribution and high frequency adjustable distribution of flow to hydraulic displacement rotary or linear motors. For this type of servo valve a patent application has been filed.
- For operation under proportional flow distribution, there is electrically powered a proportional solenoid, in order to adjust the displacement of the spool, and a solenoid type "all-or-nothing", in order to change the direction of movement.
- For operation under high frequency adjustable distribution, there is electrically powered only the small motor which drives a cam plate.
- This servo valve has some advantages relating to: simplified construction, no pressure losses in the "null position", average fineness of the hydraulic oil filtration, capability for operation as a generator of high-frequency hydraulic impulses.

REFERENCES

[1] N. Ioniţă, T.C. Popescu, L. Enache, M. Blejan, "Servovalvă hidraulică"/ *Hydraulic servo valve*, Patent Application no. A/00714/09.10.2012

EXPERIMENTAL RESEARCH ON HIGH EFFICIENCY SOLAR AIR HEATING COLLECTORS

Prof. Ph.D. Adrian CIOCANEA[1], Lect. Ph.D. Dorin Laurenţiu BUREŢEA[1]

[1] University Politehnica Bucharest, adrian.ciocanea@upb.ro

Abstract: *The paper presents a comparison between two solar air heating collectors: a single passage and a through-pass one with the same geometry, cross section and materials used. Both collectors were exposed to the sun in the same conditions of irradiation, angle of inclination, wind speed and internal air flow rate. Thermal transducers were mounted in the same position for both collectors in order to obtain the inlet temperature spectrum. According to the experimental data the through-pass collector reported a higher efficiency for the same operating conditions and a more favorable pattern for the inlet air flow. Still, the noise level due to the fan is higher in the case of the through-pass collector.*

Keywords*: solar air heating collector, solar ventilation, solar collector heat transfer*

1. Introduction

Studies concerning the efficiency of the solar air heating collectors was conducted for: (i) identifying optimal geometry and structure such as single, double or multiple pass solar air collectors ex. [1-5]; (ii) enhancing the convective heat exchange using obstacles or baffles in order to divert the flow and raise the turbulence coefficient ex. [6-9] including the influence of the roughness on heat exchange ex. [10-14]; (iii) materials and criteria for selecting them ex. [15-19]. The studies provided basic information regarding: (i) the best geometry of the collectors (ex. the optimum depth of airflow channel should be 2.5 $x10^{-3}$ times the length of the channel [1] indicating that the depth should be 2.5 mm when the length is 1 m.); (ii) optimum material selection (ex. [20] pointed out that using the solar selective coating on the absorber plate may not have significant positive impact [20]); (iii) maximum heat transfer enhancement (ex. [21] obtained good results for the effect of dimple shaped artificial roughness and [22] for multi "V" shape with a gap as the roughness element).

Starting from these points of view, the present paper presents a comparison between two types of solar heating collectors: one is a single passage collector with straight channels made of extruded aluminum, the other is a through-pass collector with a double wire net made of soft steel arranged in an "V" configuration. The analysis of the two collector efficiency was made under the same warm up conditions. The comparison between the two collector types allows calculation of the overall efficiency and the internal temperature spectrum.

2. The solar air heating collectors and setup structure

The two solar heating air collectors was manufactured with the same dimensions BxLxh = 0.7x1.4x 0.08 m - the cross section is the same - Figure nr. 1. Temperature transducers was mounted on the back side of each collector (16 pcs. /collector) in the same position and other 4 transducers was placed in the confusor section at the outlet– in the same section hummidity and pressure was measured using transduceres in order to make correction of the density of the air flow. The inclination angle for the collectors was 55^0 and the pyranometer used for measuring solar irradiation was placed also at the same inclination. The inlet air flow was provided by two fans electronically driven for a constant velocity of 1 m/s – air velocity was measured at the outlet section of the circular tube (the tube has the same cross section as the rectangular one from the inlet). Wind speed was measured with an anemometer. All the 50 parameters was sampled every 10 sec. - solar irradiation (1), humidity (2) and internal pressure (2), rotating speed of the fans (2),

inlet temperature for each collector including the confusor(20x2), wind speed (1), external temperature near esch collector (2)– Figure nr. 2.

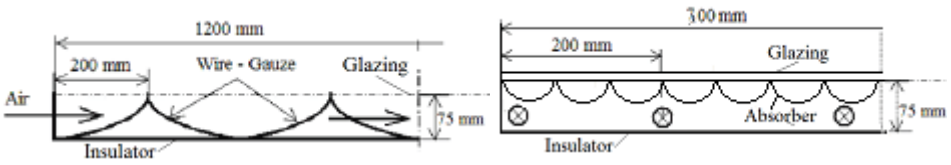

a. through-pass collector C1; b. single passage collector C2

Fig.1 Solar thermal air collectors (left: through-pass collector C1; right: single passage collector C2)
a. Shape of the through-pass collector C1; b. shape of the single-pass collector C2

Fig.2The thermal transducers for both solar thermal air collectors

The absorber for the the single pass collector is an aluminium sheet of 0.5 mm thick and for the through pass collector it was used a double leyered wire net of fine mesh of about 0,12 mm

3. Experimental research

The experiments was conducted for the warming up phase starting at the outdoor temperature t_0 =17.6^{0}C, relative humidity u_0 = 44.7 % and atmospheric pressure p_0 =1022 mbar. During the experiment the external pressure remained stable but temperature and humidity changed hence air density was re-calculated in order to derive volumetric air flow rate through the collectors. The data sampled at every 10 sec. was used for calculating the warming variation process T(t), the efficiency of the collectors η(t) and the temperature spectrum at 6 moments: at t_1= 3 min; t_2= 9 min; t_3= 17min; t_4= 56 min and t_5= 78min. In Figure nr.3 there is presented the temperature spectrum for each of the 6 moments both for single pass (C2) and through pass (C1)

collectors. The results shows that collector C1 is more efficient due to the dense wire mesh absorber which provide more effective heat transfer than the collector C2 even this one has 3 barriers. In fact, it can be seen that in the second stage of C2 in the left hand of the thermic spectrum and in the third stage on the right side there are stagnation areas. In these areas the flow section is decreasing and the air velocity is increasing hence heat transfer less efficient. On the contrary for C1 there are no such stagnant flow areas and the heat transfer is better developed.

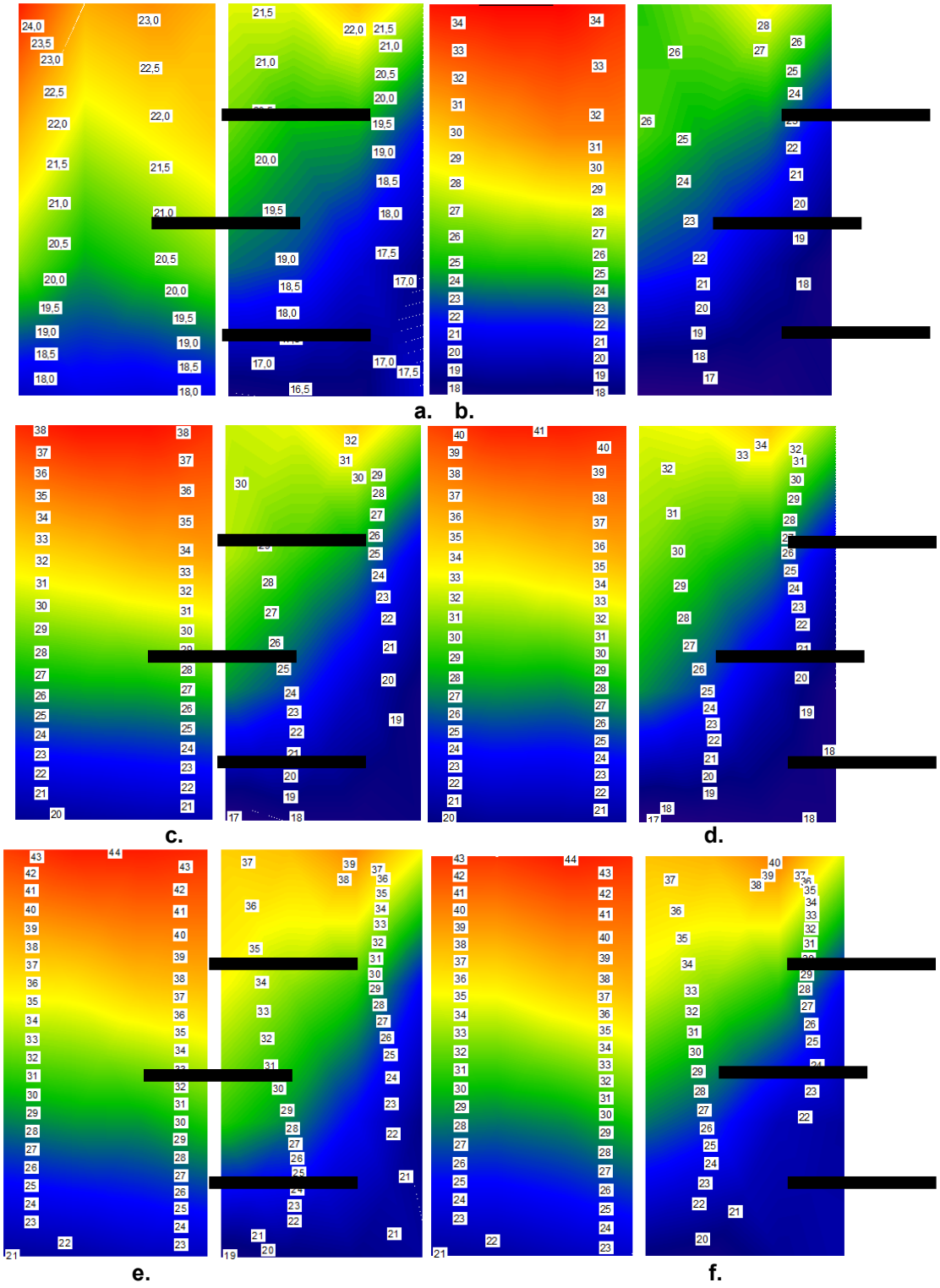

Fig.3 The thermal spectrum of the collectors at:
a. t_1= 3 min; b. t_2= 9 min; c. t_3= 17min; d. t_4= 56 min e. t_5= 78min
(left: through-pass collector C1; right: single passage collector C2)

In figure nr. 4 a,b are presented the warming up process and the overall efficiency of the collectors. The results shows a clear difference between the two collectors where C1 has a better behaviour even after 10 min form the starting moment of the testing.

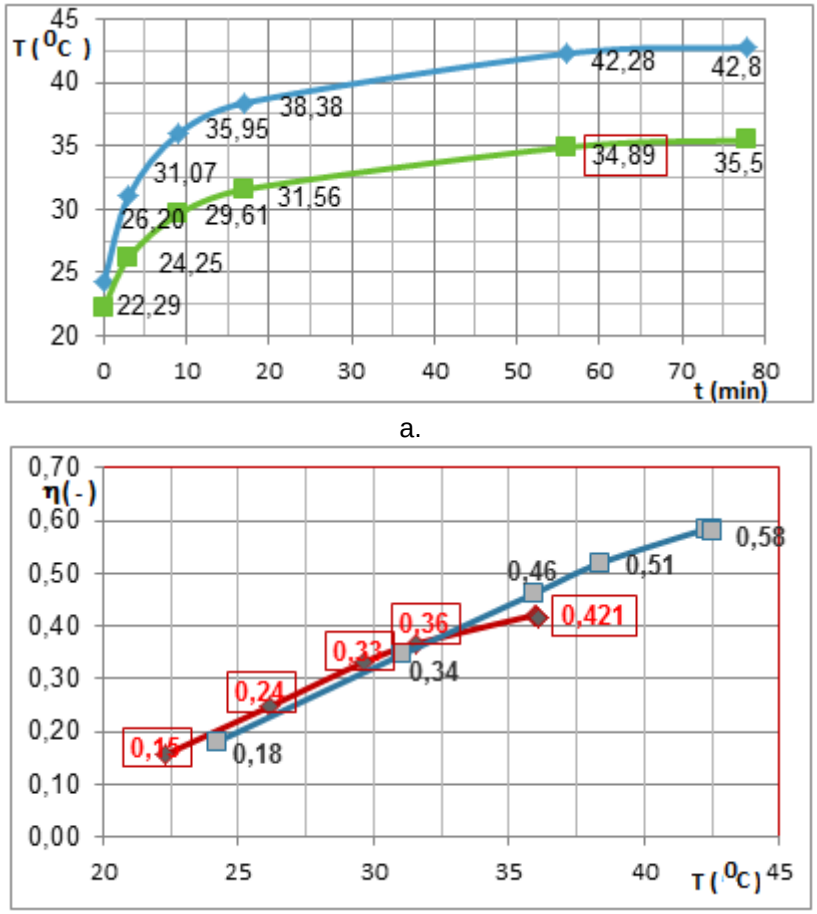

a.

Fig.4 The thermal spectrum of the collectors at:
a. Worming up process; b. Efficiency of the collectors
(blue: through-pass collector C1; red: single passage collector C2)

The results shows that the collector C1 is close to an effciency of 58% since collector C2 reaches only 42%. Also it can be seen that after 10 minutes form starting the measurement process, the temperature difference between the collector C1 and C2 is about (6-7) ^{0}C and this value is mantained for all the 78 minutes during the testing process. Since the solar irradiation was about 900-950 W/m^2 it can be accepted that in natural conditions collector C1 is more efficient than C2 collector.

Conclusions

The paper presents a comparison between two solar air heating collectors: a single passage and a through-pass one with the same geometry, cross section and materials used. According to experimental data the through-pass collector reported a higher efficiency for the same operating conditions and a more favorable pattern for the inlet air flow. The warming up process shows a better behavior for collector C1 which is reaching a higher temperature (7^0 C) then collector C2 and about 16% more in terms of overall efficiency. More research must be performed in order to develop better flow pattern inside collectors in order to enhance heat transfer.

REFERENCES

[1] Hegazy AA. Performance of flat plate solar air heaters with optimum channel geometry for constant/variable flow operation. *Energy Conversion Management*, 2000;41(4):401e17.
[2] Ming et al., 2010 Experimental analysis on thermal performance of a solar air collector with a single pass Building and Environment 56 (2012) 361e369.
[3] Parker B.F., Lindley M.R., Colliver D.G., Murphy W.E., (1993), Thermal performance of three solar air heaters, *Solar Energy*,
51, 467-479.
[4] Ramani B.M., Gupta, A., Kumar, R., (2010), Performance of a double pass solar air collector, *Solar Energy*, **84**, 1929-1937.
[5] Wijeysundera N.E., Lee Lee Ah, Lim Ek Tjioe, (1982), Thermal performance study of two pass solar air heaters, *Solar Energy*, **28**, 363-370.
[6] Abene A., Dubois V., Le Ray M., Ouagued A., (2004), Study of a solar air flat plate collector: use of obstacles and application for the drying of grape, *Journal of Food Engineering*, **65**, 15-22.
[7] Ben Slama Romdhane, (2007), The air solar collectors: Comparative study, introduction of baffles to favor the heat transfer, *Solar Energy*, **81**, 139-149.
[8] Choudhury C., Gary H. P., (1993), Performance of air heating collectors with packed airflour passage, *Solar Energy*, **50**, 205-221.
[9] Peng D., Zhang X., Dong H., Lv K., (2010), Performance study of a novel solar air collector, *Applied Thermal Engineering*, **30**, 2594-2601.
[10] Biondi P., Cicala L., Farina G., (1988), Performanceanalysis of solar air heaters of conventional design,*Solar Energy*, **41**, 101-107.
[11] El-Sawi A.M., Wifi A.S., Younan M.Y., Elsayed E.A.,Basily B.B., (2010), Application of folded sheet metalin flat bed solar air collectors, *Applied ThermalEngineering*, **30**, 864-871.
[12] Gupta D., Solanki S.C., Saini J.S., (1993), Heat and fluidflow in rectangular solar air heater ducts havingtransverse rib roughness on absorber plates, *SolarEnergy*, **51**, 31-37.
[13] Lanjewar A., Bhagoria J.L., Sarviya R.M., (2011),Experimental study of augmented heat transfer and friction in solar air heater with different orientations ofW-Rib roughness, *Experimental Thermal and Fluid Science*, **35**, 986-995.
[14] Messaoudi H., Ahmed-Zaid Le Ray M., (1997), *The role ofgeometry on improvement or reducing the exchange ofthermic turbulences in solar captors for air (inFrench)*, Proc. 3th Congress of Mechanics, TheMaroccan Society of Mechanical Sciences from theUniversity Abdelmalek Essaadi, Faculty of Science -Tetouan, , vol. **VI**, 637-644.
[15] Chiou J.P., El-Wakil M.M., Duke J.A., (1965), A slit-andexpanded aluminum-foil matrix solar collectors, *Solar Energy*, **9**, 73-80.
[16] Digel R., Fisch N., Hahne E., (1988), *High Efficiency SolarFlat Plate Collector with Capillary Structures*, In: *Advanced in Solar Energy Technology* vol. II, Bloss.
[17] Farooq M., Hutchins M.G. (2002), A novel design in composities of various materials for solar selective coatings, *Solar Energy Materials and Solar Cells*, **71**,523-535.
[18] Hachemi A., (1999), Technical note comparative study on the thermal performances of solar air heater collectors with selective absorber plate, *Renewable Energy*, **17**, 103-112.
[19] Mittal MK, Varun Saini RP, Singal SK., (2007),Effective efficiency of solar air heaters having different types of roughness elements on the absorber plate. *Energy*;32(5):739e45.
[20] Moummi N, Youcef-Ali S, Moummi A, Desmons JY., (2004), Energy analysis of a solar air collector with rows of fins. *Renewable Energy* 2004;29(13):2053e64.
[21] Saini, RP.VermaJitendra. (2008). Heattransferandfrictionfactorcorrelationsfora duct havingdimple-shapeartificial roughnessforsolarairheaters.*Energy* 2008;3:1277–87.
[22] KumarAnil,SainiR.P.,Saini, J.S., (2013), DevelopmentofcorrelationsforNusseltnumber and frictionfactorforsolarairheaterwithroughenedducthavingmultiV- shaped withgapribasartificial roughness. *Renew Energy*2013;58:151–63.


http://hidraulica.fluidas.ro